

Ronald S. Harichandran  
H. Max Irvine

MIT-7-82-004 C3

# A Static Analysis Technique for Multi-Leg Cable-Buoy Systems



MIT Sea Grant  
College Program

Massachusetts  
Institute of Technology  
Cambridge, MA 02139

MITSG 82-13  
July 1982

A STATIC ANALYSIS TECHNIQUE  
FOR MULTI-LEG CABLE-BUOY SYSTEMS

Ronald S. Harichandran  
H. Max Irvine

MIT Sea Grant  
College Program

Massachusetts  
Institute of Technology  
Cambridge, MA 02139

MITSG 82-13  
Grant NA 79AA-D-00101  
Project R/0-5  
July 1982

Abstract

A tangent stiffness technique for the static analysis of multi-leg cable-buoy systems is derived. In this procedure each cable is treated as a single element. The effect of static buoyancy on submerged cables is studied in detail. An approximate method of accounting for the current drag forces on the cables is presented. Extension of the analysis technique to more complex systems is exemplified by considering two specific systems. A possible design procedure for the location of buoys is also given.

Acknowledgements

The helpful comments of Prof. Michael S. Triantafyllou and Mr. Ralf Peek are much appreciated.

The work presented herein is the result of study sponsored by the Sea Grant Program under a NOAA Grant NA 79AA-D-00101 -- R/O-5; project title - "Mechanics of Cable Systems with Offshore Applications."

The authors are grateful to Mrs. J. Malinofsky for her patient efforts in typing the manuscript.

Table of Contents

	<u>page</u>
CHAPTER 1 - INTRODUCTION	1
CHAPTER 2 - SOLUTIONS FOR CABLES SUSPENDED IN AIR AND SUBMERGED IN WATER	3
2.1 The Symmetric Catenary	3
2.2 The Elastic Catenary	5
• Alternative formulation	9
2.3 Cables Submerged in Water	11
• Buoyancy force	11
• Buoyancy forces in finite segment modelling	15
• Equilibrium equations	15
• Differences between a submerged cable and a submerged chain	19
• Forces at the ends of cables	19
2.4 Cables in Compression	21
• Profiles of inextensible cables when compression is imminent	21
CHAPTER 3 - STATIC ANALYSIS OF SUBMERGED MULTI-LEG CABLE-BUOY SYSTEMS	27
3.1 Introduction	27
3.2 The Tangent Stiffness Matrix for a Cluster of Cables	27
3.3 Static Analysis Using a Tangent Stiffness Solution Procedure	32
3.4 Approximate Treatment of a Uniform Current Profile for Flat-Sag Cables	36
• Summary of approximate analysis under uniform current	43
3.5 Example - A Tri-moored Subsurface Buoy	44

Table of Contents (Cont.)

	Page
CHAPTER 4 - APPLICATION OF STATIC ANALYSIS PROCEDURE TO OTHER CABLE SYSTEMS	
4.1 Multi-buoy Systems	49
4.2 Moored Semisubmersibles	53
• Buoyancy effects on the rigid semi- submersible	56
• Analysis procedure	59
 REFERENCES	
 APPENDIX A. A DESIGN PROCEDURE FOR MULTI-LEG CABLE-BUOY SYSTEMS	 A1
• Outline of the problem	A1
• A preliminary design procedure	A1
 APPENDIX B. A FORTRAN COMPUTER PROGRAM	 B1
• Listing of the program	B2
• A sample output from the program	B12

List of Tables

		<u>Page</u>
2.1	Parameters of the Critical Profiles for Various Values of $\frac{z_0}{l/2}$ .	26

List of Figures

<u>Fig. No.</u>	<u>Title</u>	<u>Page</u>
2.1	Definition Diagram for Cable and Forces Acting on an Infinitesimal Element	4
2.2	Coordinates for the Elastic Catenary and Forces on a Segment of the Strained Cable Profile	5
2.3	Forces Acting on an Infinitesimal Element of the Elastic Catenary	10
2.4	Illustrations for an Element from a Submerged Cable	13
2.5	Buoyancy Effects in Finite Segment Models	16
2.6	Forces at the Ends of a Cable	20
2.7	Submerged Cables in Compression	20
2.8	Definition Diagram for the Class of Profiles Being Studied	23
2.9	Plot of $\frac{l/2}{d}$ vs. $\frac{z_0}{d}$ for the limiting Profiles	25
3.1	Illustrations for Derivation of Tangent Stiffness Matrices	28
3.2	One-dimensional Representation of Solution Techniques	33
3.3	Drag Forces on a Cable Element	38
3.4	In-plane Loading on an Inclined Flat-sag Cable	38
3.5	Displacements of an Element of the Cable	38
3.6	End Forces Due to Self Weight Only	42

List of Figures (Cont.)

<u>Fig. No.</u>	<u>Title</u>	<u>Page</u>
3.7	A Typical Cable Cluster	42
3.8	Definition Diagram for Numerical Example	45
4.1	Two-buoy System	50
4.2	Rectangular Moored Semisubmersible	54
4.2	Buoyancy Effects on the Semisubmersible	57
A.1	Definition Diagram for Typical Cables	A2



## CHAPTER 1 - INTRODUCTION

Surface-moored buoys in the oceans have been used over many centuries for marking, mooring and navigational purposes. In recent years fully submerged buoys and their mooring lines have found increasing use as stable platforms to support various current meters and sensors for scientific purposes. For such systems it is important to control the excursions of the buoys under the influence of ocean currents. This work deals primarily with the static analysis of multi-leg cable-buoy systems.

A system consisting of a surface-moored or submerged buoy secured to the ocean floor by many cables is, in general, nonlinear in its load-deflection behavior. Analytical solutions are thus intractable except for special cases where the cables are sufficiently taut and flat such that the system behavior is essentially linear. Numerical methods for the solution of the more general systems have been developed in recent years. Most of these use finite segment modelling techniques (e.g., Skop and O'Hara, 1970), and hence allow for variable properties and arbitrary drag force distributions along the cables. The method developed herein is more simplistic, requiring uniform cables and a uniform current velocity with depth. However, it possesses the advantage of treating each cable as a single element and thus requires minimal storage capacity, enabling it to be implemented in mini-computers that have limited storage capabilities.

The basic properties and equilibrium configurations of cables suspended in air are derived in the first two sections of Chapter 2. A detailed study of the buoyancy forces on submerged cables and the resulting equilibrium profiles are presented in the third section. It is shown that inextensible or incompressible cables have the same profile in water as they do in air, but that the tensions in the cables are different. The fundamental difference between the behavior of submerged chains and submerged cables is identified. It is shown in the fourth section that it is possible for some submerged cables to be in a state of axial compression.

A static analysis technique for submerged multi-leg cable-buoy systems is developed in Chapter 3. The method is an adaptation of a standard tangent stiffness solution procedure for nonlinear structural systems. The results from the analysis are "exact" when the only lateral load acting is that on the buoy. The approximate treatment of drag forces on the cables due to a uniform current profile is presented in the fourth section (for relatively flat-sag cables). The final section consists of an example illustrating the solution procedure.

Application of the static analysis procedure developed in Chapter 3 to more complicated floating cable systems is discussed in Chapter 4. The tangent stiffness matrix required for the analysis is derived for two specific systems: a multi-buoy system and a moored semisubmersible.

Finally, a possible design procedure to locate anchor points on the seabed and determine the cable dimensions such that the buoy is positioned at the prescribed location, is briefly discussed in Appendix A.

CHAPTER 2

SOLUTIONS FOR CABLES SUSPENDED IN AIR AND SUBMERGED IN WATER

2.1 The Symmetric Catenary

Consider a uniform inextensible cable, or chain, suspended in air between two points at the same level. The cable is assumed to be devoid of flexural rigidity and able to sustain only tension forces. Referring to Fig. 2.1, vertical equilibrium of the isolated element of the cable located at  $(x,z)$  requires that (Irvine, 1981):

$$\frac{d}{ds} \left( T \frac{dz}{ds} \right) = - mg \quad (2.1)$$

where  $T$  is the tension in the cable,  $dz/ds$  is the sine of the angle subtended to the horizontal by the tangent to the profile, and  $mg$  is the self-weight of the cable per unit length. Horizontal equilibrium yields

$$\frac{d}{ds} \left( T \frac{dx}{ds} \right) = 0 \quad (2.2)$$

where  $dx/ds$  is the cosine of the angle of inclination. Equation (2.2) may be directly integrated to give

$$T \frac{dx}{ds} = H \quad (2.3)$$

where  $H$  is the horizontal component of the tension and is constant everywhere since no longitudinal loads are acting on the cable. Equation (2.1) may thus be reduced to

$$H \frac{d^2z}{dx^2} = - mg \frac{ds}{dx} \quad (2.4)$$

Note that when  $mg \frac{ds}{dx}$ , the intensity of load per unit horizontal length, is constant, the resulting cable profile is parabolic. Using the geometric constraint

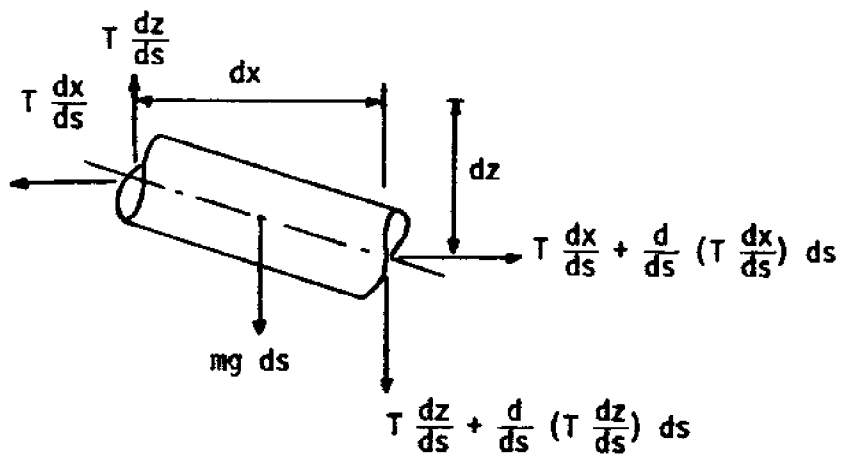


Fig. 2.1 - Definition Diagram for Cable and Forces Acting on an Infinitesimal Element

$$\left(\frac{dx}{ds}\right)^2 + \left(\frac{dy}{ds}\right)^2 = 1 \quad (2.5)$$

the governing differential equation of the catenary takes the form

$$H \frac{d^2z}{dx^2} = -mg \left\{ 1 + \left(\frac{dz}{dx}\right)^2 \right\}^{1/2} \quad (2.6)$$

The solution that satisfies equation (2.6) and the boundary conditions is

$$z = \frac{H}{mg} \left\{ \cosh \left(\frac{mgx}{2H}\right) - \cosh \frac{mg}{H} \left(\frac{\ell}{2} - x\right) \right\} \quad (2.7)$$

An expression for the length of a portion of the cable is

$$s = \int_0^x \left\{ 1 + \left(\frac{dz}{dx}\right)^2 \right\}^{1/2} dx = \frac{H}{mg} \left\{ \sinh \left(\frac{mgx}{2H}\right) - \sinh \frac{mg}{H} \left(\frac{\ell}{2} - x\right) \right\} \quad (2.8)$$

so that, if a cable of length  $L_0$  is used to span between the supports, the horizontal component of cable tension may be found by solving

$$\sinh \left(\frac{mgx}{2H}\right) = \frac{mgL_0}{2H} \quad (2.9)$$

for  $H$ . Note that for the inextensible cable a solution cannot exist if  $L_0$  is not greater than  $\ell$ . The tension at any point is given by

$$T = H \cosh \frac{mg}{H} \left(\frac{\ell}{2} - x\right) \quad (2.10)$$

## 2.2 The Elastic Catenary

The profile of a suspended cable, when elastic stretch is taken into account, is the elastic catenary. For this case it is convenient to adopt a Lagrangian approach.

The cable shown in Fig. 2.2 is suspended between two fixed points A and B which have Cartesian coordinates (0,0) and ( $\ell$ ,h) respectively.

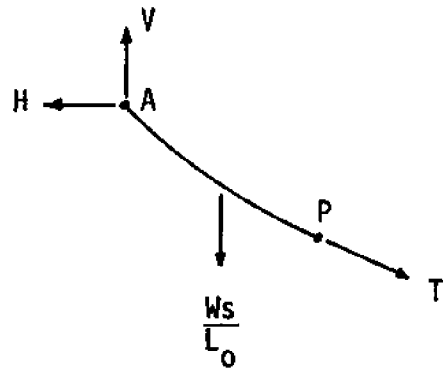
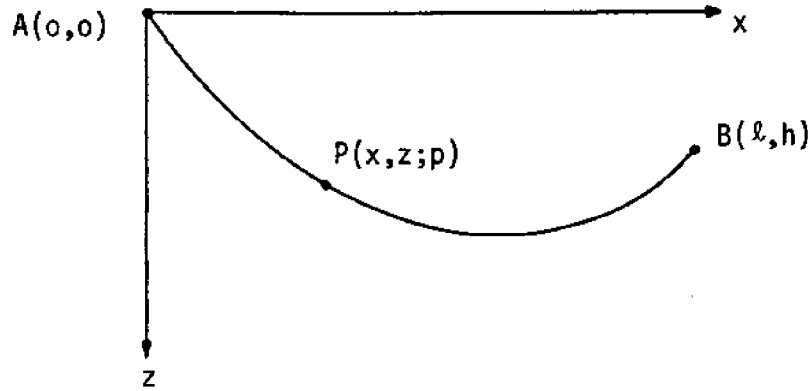


Fig. 2.2 - Coordinates for the Elastic Catenary and Forces on a Segment of the Strained Cable Profile

The unstrained length of the cable is  $L_0$ . A point on the cable has Lagrangian coordinate  $s$  in the unstrained profile (i.e., the length of cable from the origin to that point is  $s$  when the cable is unloaded). Under the self-weight of  $W (= mgL_0)$  this point moves to occupy its new position in the strained profile described by Cartesian coordinates  $x$  and  $y$  and Lagrangian coordinate  $p$ .

The geometric constraint to be satisfied is

$$\left(\frac{dx}{dp}\right)^2 + \left(\frac{dz}{dp}\right)^2 = 1 \quad (2.11)$$

while, with reference to Fig. 2.2, the balancing of horizontal and vertical forces yield

$$\begin{aligned} T \frac{dx}{dp} &= H \\ T \frac{dz}{dp} &= V - W \frac{s}{L_0} \end{aligned} \quad (2.12)$$

Due to conservation of mass, the weight of that portion of the strained profile shown in the figure is simply  $Ws/L_0$ . The vertical reaction at the support is  $V$ , and as before  $H$  is the constant horizontal component of cable tension. A constitutive relation that is a mathematically consistent expression of Hooke's law is

$$T = EA_0 \left(\frac{dp}{ds} - 1\right) \quad (2.13)$$

where  $E$  is Young's modulus and  $A_0$  is the uniform cross-sectional area in the unstrained profile.

The end conditions at the cable supports A and B are

$$\begin{aligned} x = 0, & \quad z = 0, & \quad p = 0 & \quad \text{at } s = 0 \\ x = \lambda, & \quad z = h, & \quad p = L & \quad \text{at } s = L_0 \end{aligned} \quad (2.14)$$

where  $L$  is the length of the cable in the strained profile.

The solutions of interest are those for  $x$ ,  $z$  and  $T$  as functions of the independent variable  $s$ .

1. Solutions for  $T = T(s)$  :

If equations (2.12) are squared and added, then using equation (2.11)

$$T(s) = \left\{ H^2 + (V - W \frac{s}{L_0})^2 \right\}^{1/2} \quad (2.15)$$

2. Solution for  $x = x(s)$ :

Note that  $\frac{dx}{ds} = \frac{dx}{dp} \cdot \frac{dp}{ds}$  and  $dx/dp$  is given as a function of  $T$  in the first equation of (2.12), while  $dp/ds$  may also be obtained as a function of  $T$  from (2.13). Hence substituting for  $T$  from (2.15) yields

$$\frac{dx}{ds} = \frac{H}{EA_0} + \frac{H}{\left\{ H^2 + (V - Ws/L_0)^2 \right\}^{1/2}} \quad (2.16)$$

Using the end condition  $x = 0$  at  $s = 0$ , this can be integrated to

$$x(s) = \frac{Hs}{EA_0} + \frac{HL_0}{W} \left\{ \sinh^{-1} \left( \frac{V}{H} \right) - \sinh^{-1} \left( \frac{V - Ws/L_0}{H} \right) \right\} \quad (2.17)$$

3. Solution for  $z = z(s)$ :

Following a procedure analogous to that employed for  $x$ ,

$$z(s) = \frac{W}{EA_0} \left( \frac{V}{W} - \frac{s}{2L_0} \right) + \frac{HL_0}{W} \left[ \left\{ 1 + \left( \frac{V}{H} \right)^2 \right\}^{1/2} - \left\{ 1 + \left( \frac{V - Ws/L_0}{H} \right)^2 \right\}^{1/2} \right] \quad (2.18)$$

4. Solutions for  $H$  and  $V$ :

In deriving the solutions for  $x$  and  $z$ , only the end conditions at  $s = 0$  in (2.14) were used. By satisfying the other end conditions for  $x$  and  $z$ , the following equations are obtained:

$$l = \frac{HL_0}{EA_0} + \frac{HL_0}{W} \left\{ \sinh^{-1} \left( \frac{V}{H} \right) - \sinh^{-1} \left( \frac{V - W}{H} \right) \right\} \quad (2.19)$$



$$h = \frac{WL_0}{EA_0} \left( \frac{V}{W} - \frac{1}{2} \right) + \frac{HL_0}{W} \left[ \left\{ 1 + \left( \frac{V}{H} \right)^2 \right\}^{1/2} - \left\{ 1 + \left( \frac{V-W}{H} \right)^2 \right\}^{1/2} \right] \quad (2.20)$$

The simultaneous solution of these equations for H and V then allows x, z and T to be evaluated. In general these equations can be solved only numerically.

The solutions for an inextensible cable may be obtained by simply neglecting all the terms containing  $\frac{1}{EA_0}$  (i.e.,  $EA_0 \rightarrow \infty$ ) in equations (2.15) to (2.20).

### Alternative formulation

An alternative formulation for the elastic catenary may be obtained by considering an infinitesimal element. The forces acting on an element located at (x,z) are shown in Fig. 2.3. The length of the element in the strained profile is dp and its weight is wdp. The angle subtended by the tangent to the cable at (x,z) to the horizontal is  $\phi$ . In the limit the sine and cosine of the incremental angle  $\frac{\partial \phi}{\partial p} \cdot dp$  become:

$$\sin \left( \frac{\partial \phi}{\partial p} dp \right) = \frac{\partial \phi}{\partial p} dp \quad (2.21)$$

$$\cos \left( \frac{\partial \phi}{\partial p} dp \right) = 1$$

Using these, the equations of equilibrium in the tangential and normal directions at (x,z) are

$$\frac{\partial T}{\partial p} + w \sin \phi = 0 \quad (2.22)$$

$$T \frac{\partial \phi}{\partial p} + w \cos \phi = 0$$

Conservation of mass gives

$$wdp = mg ds \quad (2.23)$$

where ds is the unstrained length of the element. Multiplying the

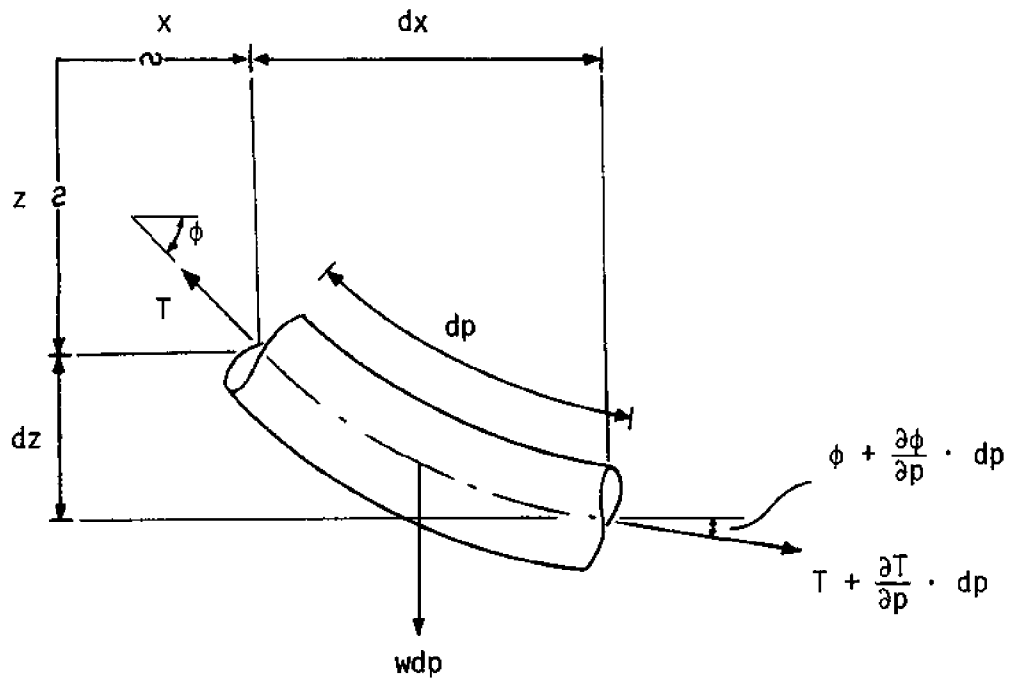


Fig. 2.3 - Forces Acting on an Infinitesimal Element of the Elastic Catenary

equations of (2.22) by  $\frac{dp}{ds}$  and using (2.23), the equilibrium equations in terms of the Lagrangian coordinate in the unstrained profile,  $s$ , are

$$\begin{aligned}\frac{\partial T}{\partial s} + mg \sin \phi &= 0 \\ T \frac{\partial \phi}{\partial s} + mg \cos \phi &= 0\end{aligned}\tag{2.24}$$

Note that for the orientation of the coordinate axes shown in Fig. 2.3 the quantities  $\frac{\partial \phi}{\partial p}$  and  $\frac{\partial \phi}{\partial s}$  are negative.

For an inextensible cable, only the boundary conditions at the two ends are required to be satisfied by the solution of the equations of (2.24). For an elastic cable, in addition to the boundary condition, Hooke's law (equation (2.13)) also needs to be satisfied.

This latter formulation will be used in the next section to obtain the equilibrium equations for a cable submerged in water.

## 2.3 Cables Submerged in Water

### Buoyancy force

It is well known that a body submerged in water has, in addition to its weight, a buoyancy force acting on it. By Archimedes' Principle this buoyancy force is equal to the weight of water displaced by the submerged body and acts vertically upwards. However, this is the case only when a partially or fully submerged body has all of its submerged surface area exposed to the water. It is often claimed that the buoyancy force on an element of a fully submerged cable acts vertically upward and is equal to the weight of water displaced by the element, but this is not so. In isolating an element from a submerged cable, the cuts made on the cable are fictitious and no pressure forces act on the surface area exposed by these cuts. It was shown by Goodman and Breslin (1976) that the buoyancy force on the element acts in a direction normal to it and is dependent not only on the weight of water it displaces, but also on its inclination to the horizontal, its depth below the free surface of the water, and its curvature.

Fig. 2.4(a) shows an element located at  $(x,z)$  in a fully submerged cable. The origin of the coordinate axes is located, as before, at the end of the cable that is at the higher level. The free surface of the water is assumed to be at the level  $z = -z_0$ , where  $z_0 \geq 0$ . If the ends of the element are exposed to the water, then the buoyancy force on the element is equal to the weight of water displaced and acts vertically upward. The actual buoyancy force on the element may be found by subtracting the pressure forces acting on the ends of the element from this force.

It is convenient here to use the Lagrangian coordinates  $p$  and  $s$  in the strained and unstrained profiles. The angle subtended by the tangent to the cable at  $(x,z)$  to the horizontal is  $\phi$ . The tangent and normal unit vectors at  $p$  are denoted by  $\hat{t}(p)$  and  $\hat{n}(p)$  respectively, and the unit vectors in the  $x$  and  $z$  directions are  $\hat{i}$  and  $\hat{k}$ . The buoyancy force on the cable element is thus

$$\begin{aligned} \vec{F} &= \gamma A \left[ -\Delta p \hat{k} - \left\{ (z+z_0) \hat{t}(p) - (z+z_0 + \Delta z) \hat{t}(p+\Delta p) \right\} \right] \\ &= \gamma A \left[ -\hat{k} + \frac{(z+z_0 + \Delta z) \hat{t}(p+\Delta p) - (z+z_0) \hat{t}(p)}{\Delta p} \right] \Delta p \end{aligned}$$

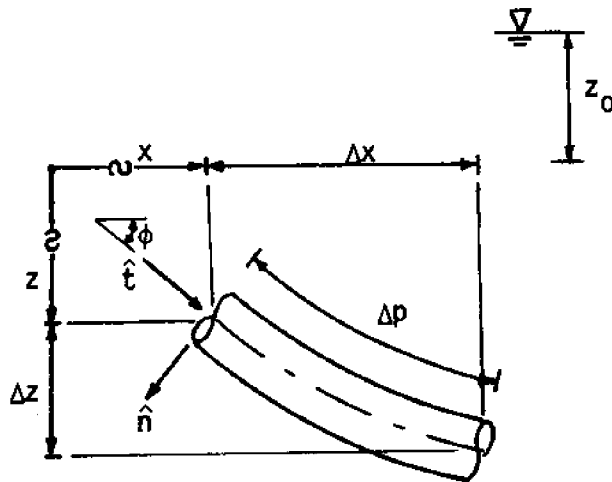
where  $\gamma$  is the weight of a unit volume of water and  $A$  is the cross-sectional area of the cable in the strained profile.

In the limit as  $\Delta p \rightarrow 0$  this becomes

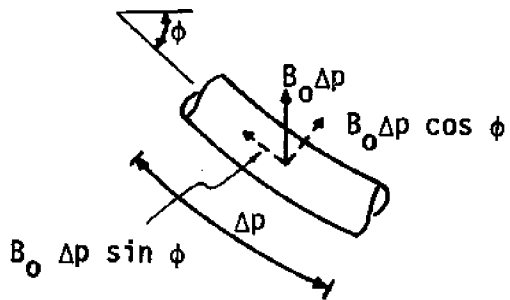
$$\vec{F} = \gamma A \left[ -\hat{k} + \frac{\partial}{\partial p} \left\{ (z+z_0) \hat{t} \right\} \right] \quad (2.25)$$

The unit tangent and normal vectors may be expressed in terms of  $\phi$  as follows:

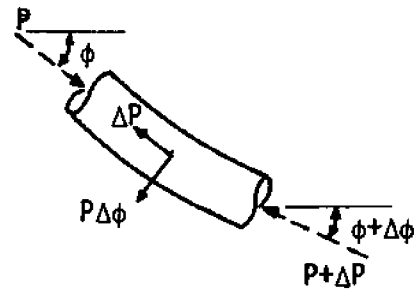
$$\begin{aligned} \hat{t} &= \cos \phi \hat{i} + \sin \phi \hat{k} \\ \hat{n} &= \frac{d\hat{t}}{d\phi} = -\sin \phi \hat{i} + \cos \phi \hat{k} \end{aligned} \quad (2.26)$$



(a) Definition Diagram



(i) Element fully exposed to water



(ii) Resultant force from pressure forces on ends.

(b) Buoyancy effects on a curved element.

Fig. 2.4 - Illustrations for an Element from a Submerged Cable

Hence,

$$\begin{aligned} \frac{\partial}{\partial p} \left\{ (z+z_0) \hat{t} \right\} &= \frac{\partial z}{\partial p} \hat{t} + (z+z_0) \frac{\partial \hat{t}}{\partial p} \\ &= \frac{\partial z}{\partial p} \hat{t} + (z+z_0) \frac{\partial \hat{t}}{\partial \phi} \frac{\partial \phi}{\partial p} \\ &= \sin \phi (\cos \phi \hat{i} + \sin \phi \hat{k}) \\ &\quad + (z+z_0) (-\sin \phi \hat{i} + \cos \phi \hat{k}) \frac{\partial \phi}{\partial p} \end{aligned}$$

Substituting this into (2.25) and noting that  $1 - \sin^2 \phi = \cos^2 \phi$

$$\begin{aligned} \frac{F}{dp} &= \gamma A \left\{ -\cos \phi + (z+z_0) \frac{\partial \phi}{\partial p} \right\} (-\sin \phi \hat{i} + \cos \phi \hat{k}) \\ &= -\gamma A \left\{ \cos \phi - (z+z_0) \frac{\partial \phi}{\partial p} \right\} \hat{n} \end{aligned} \quad (2.27)$$

Thus, as stated before, the buoyancy force on an element depends on its inclination  $\phi$ , its depth  $(z+z_0)$  and its curvature  $\frac{\partial \phi}{\partial p}$  and is directed in a direction normal to the cable.

A heuristic but more physical approach of computing the buoyancy force on an element is as follows. Consider the curved element shown in Fig. 2.4(b). The buoyancy force on the element if the ends of the element were exposed to water is shown on the left. The vertical buoyancy force can be resolved into tangential and normal components  $B_0 \Delta p \sin \phi$  and  $B_0 \Delta p \cos \phi$  respectively. The resultant force on the element due to the pressure forces on the ends is shown on the right, and both tangential and normal resultants  $\Delta P$  and  $P\Delta\phi$  (neglecting second order terms) exist. The pressure forces on the sides of the element are essentially normal to the cable axis. Since the total normal force on the element is  $B_0 \Delta p \cos \phi$ , the resultant of the pressure forces acting on the sides of the element is  $B_0 \Delta p \cos \phi + P\Delta\phi$ . If there were no pressure forces on the ends of the element, then this normal component

would be the only force present due to buoyancy. In the limit, the buoyancy force per unit length is  $B_0 \cos \phi + P \frac{\partial \phi}{\partial p}$ , where  $P = \gamma A z$  and  $B_0 = \gamma A$ , yielding the same result as that obtained previously by more rigorous means.

### Buoyancy forces in finite segment modelling

Many numerical techniques for the static and dynamic analysis of cable systems approximate the cables as finite segment models (see Fig. 2.5(a)). In such models each segment is assumed to be straight (i.e., zero curvature) so that the uniformly distributed normal buoyancy force along its length is simply  $\gamma A \cos \phi$ , where  $\phi$  is the angle of the axis of the segment to the horizontal. The buoyancy contributions due to curvature (which have been overlooked by some authors) appear as concentrated forces at the segment junctions.

Consider the corner element  $B B_1 B_2$  of Fig. 2.5(b). The vertical buoyancy force if the faces  $B B_1$  and  $B B_2$  were exposed to the water would be  $-\gamma V_e \hat{k}$  where  $V_e$  is the volume of the element. The concentrated buoyancy force at  $B$ ,  $F_i$ , can be obtained by subtracting (vectorially) the non-existent pressure forces in the end forces from  $-\gamma V_e \hat{k}$ . For most practical purposes the volume of the corner element may be neglected, in which case  $F_i = 2\gamma A(z_i + z_0) \sin(\frac{\Delta\phi}{2}) \approx \gamma A(z_i + z_0)\Delta\phi$ , where  $z_i$ ,  $z_0$  and  $\Delta\phi$  are as defined in Fig. 2.5 and  $\Delta\phi$  is assumed to be small. The force  $F_i$  bisects the angle  $ABC$  between the adjacent segments of the cable.

### Equilibrium equations

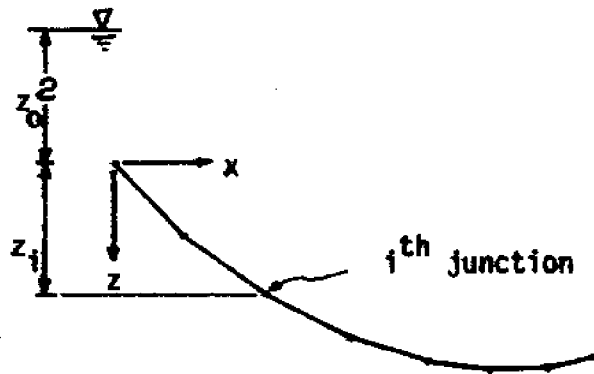
The equilibrium equations for the element may be obtained by adding the buoyancy term into the second equation of (2.22) to yield

$$\frac{\partial T}{\partial p} + w \sin \phi = 0$$

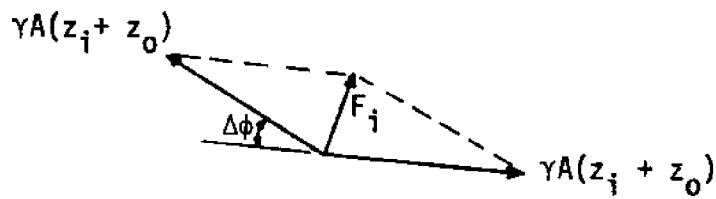
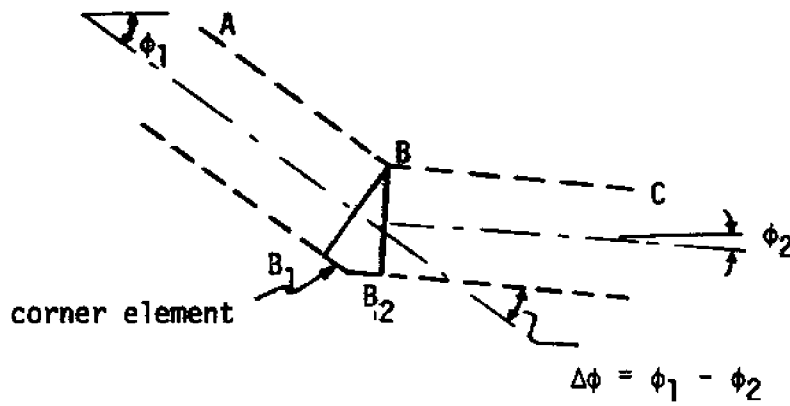
$$\left\{ T + \gamma A(z+z_0) \right\} \frac{\partial \phi}{\partial p} + (w - \gamma A) \cos \phi = 0$$

(2.28)

Goodman and Breslin (1976) first demonstrated the considerable simplifications obtained by introducing the "effective tension" defined as



(a) Finite segment model of a cable



(v) The  $i^{\text{th}}$  junction

Fig. 2.5 - Buoyancy Effects in Finite Segment Models



$$T_e = T + \gamma A(z+z_0) \quad (2.29)$$

Using the fact that  $dz/dp = \sin \phi$ , the equations of (2.28) in terms of  $T_e$  are

$$\frac{\partial T_e}{\partial p} + (w - \gamma A) \sin \phi = 0 \quad (2.30)$$

$$T_e \frac{\partial \phi}{\partial p} + (w - \gamma A) \cos \phi = 0$$

Multiplying the above equations by  $\frac{dp}{ds}$  and observing that  $w \frac{dp}{ds} = mg$  and  $A \frac{dp}{ds} = A_0$  (the cross-sectional area of the unstrained cable), the equilibrium equations in terms of  $s$  are found to be

$$\frac{\partial T_e}{\partial s} + (mg - \gamma A_0) \sin \phi = 0 \quad (2.31)$$

$$T_e \frac{\partial \phi}{\partial s} + (mg - \gamma A_0) \cos \phi = 0$$

The similarity of the above equations to the equations of (2.24) suggests that for an inextensible cable, the profile in water is also a catenary and the required solutions may be obtained by replacing  $W = mgL_0$  by  $W' = (mg - \gamma A_0) L_0$  in equations (2.15) to (2.20) with  $EA_0 \rightarrow \infty$ . However, the tensions and the end forces computed from equations (2.15), (2.19) and (2.20) will be the effective forces and not the actual forces. The actual tension is obtained by using equation (2.29). If an end of the cable is fixed to a point on the free surface of the water (i.e.,  $z = z_0 = 0$ ), then at that point the effective tension and the actual tension are identical. Equation (2.29) also suggests that if the cable extends to a depth  $z$  where  $\gamma Az$  is greater than  $T_e$ , then it is required to carry compressive forces. This aspect will be discussed in more detail in Section 2.4.

For an extensible cable, in addition to the equilibrium equations the equations of elasticity also need to be satisfied. Consider again the element of the submerged cable located at  $(x,z)$ . In addition to the tensile forces acting in the longitudinal direction, the element is also subjected to lateral hydrostatic pressure forces. In cylindrical coor-

ordinates  $(r, \theta, z)$ , the stresses at the point  $(x, z)$  are

$$\begin{aligned} \sigma_r = \sigma_\theta &= -\gamma(z+z_0) \\ \sigma_z &= \frac{T}{A_0} \end{aligned} \tag{2.32}$$

Assuming that the cable is a linear elastic solid with Young's modulus  $E$  and Poisson's ratio  $\nu$ , the longitudinal strain of the element is

$$\begin{aligned} \epsilon_z &= \frac{dp}{ds} - 1 = \frac{1}{E} \left\{ \frac{T}{A_0} + 2\nu\gamma(z+z_0) \right\} \\ &= \frac{1}{E} \left\{ \frac{T_e}{A_0} + \gamma(z+z_0)(2\nu - \frac{A}{A_0}) \right\} \end{aligned} \tag{2.33}$$

The solution of equations (2.31) and (2.33) is complicated by the appearance of  $z$  in the above equation. However, an interesting result is obtained for an incompressible cable for which  $\nu = 1/2$ .

Since  $\frac{A}{A_0} = \frac{ds}{dp} \approx 1$ , equation (2.33) may be reduced to

$$\frac{dp}{ds} - 1 \approx \frac{T_e}{EA_0}$$

or 
$$T_e \approx EA_0 \left( \frac{dp}{ds} - 1 \right) \tag{2.34}$$

The equations governing the submerged incompressible cable are now identical to the equations for an extensible cable suspended in air (equations (2.24) and (2.13)) with the weight of the cable,  $mg$ , replaced by  $(mg - \gamma A_0)$  and the cable tension  $T$  replaced by  $T_e$ . Thus it may be deduced that the profile of the cable is approximately an elastic catenary. The solutions for  $x$ ,  $z$  and  $T_e$  may be obtained from equations (2.15) to (2.20). As for the inextensible cable, the real tensions may be computed from  $T_e$  using (2.29).

### Differences between a submerged cable and a submerged chain

A rather subtle point that is worth noting here is the basic difference between the behavior of a submerged inextensible cable and a submerged inextensible chain. For an ideal chain, two adjoining links touch only at a point. Hence each link is essentially completely exposed to water, and the buoyancy force on it acts vertically upwards. Globally the chain may be assumed to behave like a cable with a reduced weight of  $W' = mg - B_0$ , where  $B_0$  is the vertical buoyancy force per unit length of the chain. The tensions and end forces computed from equations (2.15), (2.19) and (2.20) would in this case be the actual forces.

The simplification that occurred for an incompressible cable does not apply for an incompressible chain for which equation (2.34) holds, but equations (2.31) do not. The equilibrium equations for this case are obtained by replacing  $mg$  in (2.24) by  $(mg - B_0)$ , where  $B_0$  is the vertical buoyancy force per unit length of chain.

### Forces at the ends of cables

It is convenient to idealize the connections at the ends of the cables as shown in Fig. 2.6. The cable is assumed to be attached to the buoy or the seabed by an infinitesimally thin strand. Pressure forces directed along the cable axis exist at the ends of the cable. Thus, if the tension in the cable at point  $a$  is  $T_a$ , then the tension  $T_1$  in the strand is  $T_1 = T_a + \gamma A z_0$ . Similarly at  $b$ ,  $T_2 = T_b + \gamma A (z_0 + z_b)$ . By comparing these expressions with equation (2.29) it can be seen that  $T_1$  and  $T_2$  are the effective tensions at  $a$  and  $b$ . For realistic connection details, localized forces and moments may exist in the connection, but the resultant force exerted on the buoy (or the seabed) is still the effective tensions. Hence the force resisting external forces on the buoy is the effective tension and not the real tension in the cable.

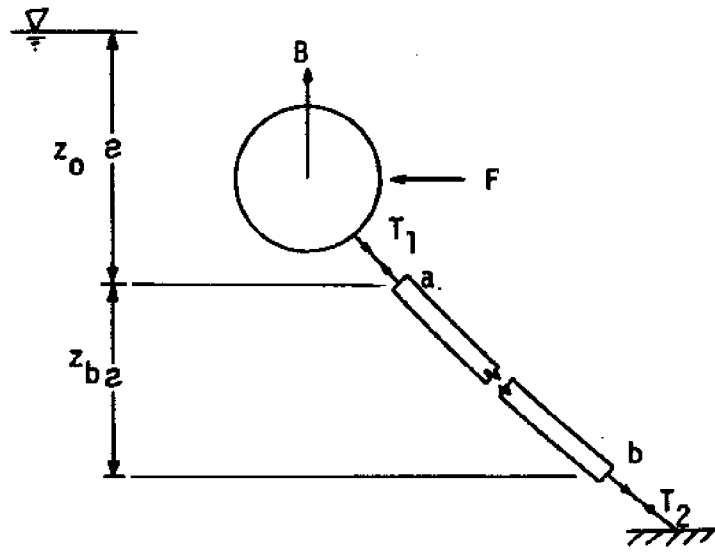
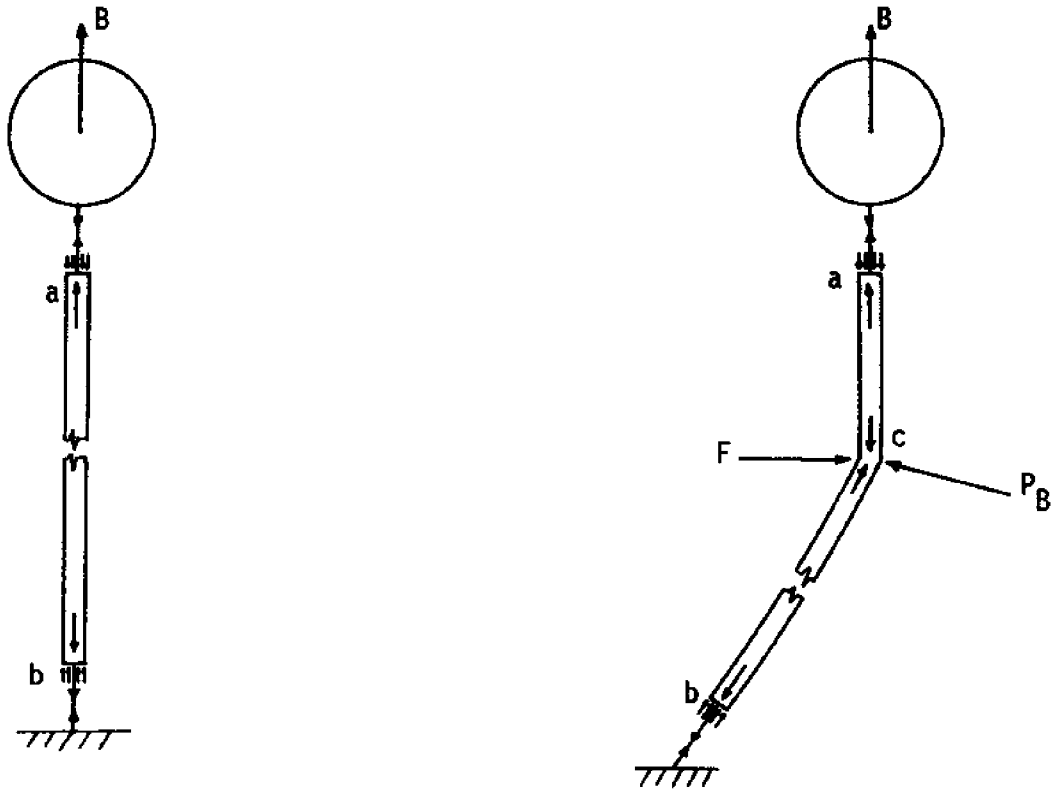


Fig. 2.6 - Forces at the Ends of a Cable



(a) Vertical buoyant force only      (b) Horizontal force on cable

Fig. 2.7 - Submerged Cables in Compression

## 2.4 Cables in Compression

It is commonly assumed that cables cannot sustain compression. However, when sufficiently large lateral confining pressures are present, cables are able to carry compressive forces (e.g., a long slender reinforcing bar in a reinforced concrete column). In the case of a cable submerged in sufficiently deep water, the effective tension in it can be smaller than the quantity  $\gamma A(z+z_0)$  so that, by equation (2.29), the actual tension in the cable is less than zero (i.e., the cable is in compression). Note, however, that for incompressible cables the axial strain is proportional to the effective tension and not the real tension. Thus, although the cable may be in compression, the lateral hydrostatic pressure is large enough such that the "squeezing" action due to it produces positive axial strains.

As an example consider a buoy moored by a single cable in deep water as shown in Fig. 2.7(a). It is assumed that the pressure force on the upper end of the cable is larger than the total upward force  $B$  on the buoy. The cable is thus in compression at point  $a$  and the compressive force increases along the cable due to its self-weight.

Now consider a lateral force  $F$  applied on the cable (as in Fig. 2.7(b)). The presence of the (pressure-induced) concentrated force  $P_B$  enables point  $c$  in the cable to be in equilibrium. Note that although the configurations shown in Fig. 2.7 satisfy equilibrium and on intuitive grounds seem correct, they may not be stable configurations. A rigorous stability analysis will not be attempted here.

### Profiles of inextensible cables when compression is imminent

As mentioned in the previous section, submerged inextensible cables have catenary profiles. The smallest tension in such a cable occurs at the point of relative minimum of the catenary. The relative dimensions of the catenary profiles to the depth of submergence are examined here to find the profiles of cables that have compression imminent in them. This is, however, not a critical condition, since it is believed that the cables are able to sustain this compression.

Consider the inextensible cable depicted in Fig. 2.8. The actual tension at any point of the cable is given by

$$T = T_e - \gamma A(z+z_0) \quad (2.35)$$

where (see Section 2.1)

$$T_e = H_e \cosh \left\{ \frac{mg - \gamma A}{H_e} \left( \frac{\ell}{2} - x \right) \right\} \quad (2.36)$$

and  $H_e$  is the solution of

$$\sinh \left\{ \frac{(mg - \gamma A)\ell}{2H_e} \right\} = \frac{(mg - \gamma A)L_0}{2H_e} \quad (2.37)$$

Also, from equation (2.7)

$$d = \frac{H_e}{mg} \cosh \left\{ \frac{(mg - \gamma A)\ell}{2H_e} \right\} \quad (2.38)$$

The value of  $T_e$  is smallest and  $(z+z_0)$  is largest at point B. Hence from (2.35) the real tension in the cable attains a minimum value at B and is given by

$$T_{\min} = H_e - \gamma A (d + z_0) \quad (2.39)$$

The limiting profiles for which  $T_{\min}$  is just equal to zero are of interest.

For a study of the parameters defining the critical profiles, it is advantageous to use nondimensional variables. Noting that

$$\frac{mg}{\gamma A} = \frac{\rho_s Ag}{\rho_w Ag} = \frac{\rho_s}{\rho_w}, \text{ where } \rho_s \text{ is the density of the cable (typically steel)}$$

and  $\rho_w$  is the density of the water, equations (2.37) and (2.38) may be written as

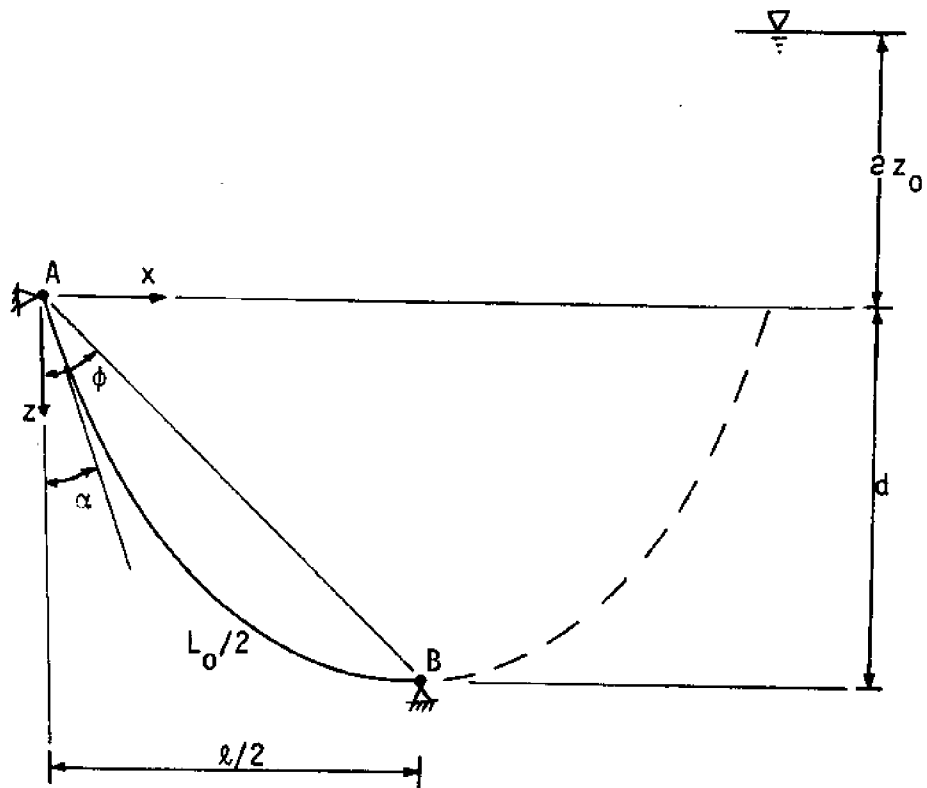


Fig. 2.8 - Definition Diagram for the Class of Profiles Being Studied

$$\sinh \beta = \beta \frac{L_0}{\ell} \quad (2.40)$$

$$\frac{\ell/2}{d} = \frac{\beta}{\cosh \beta - 1} \quad (2.41)$$

where

$$\beta = \frac{\left(\frac{\rho_s}{\rho_w} - 1\right) \frac{\ell/2}{(d+z_0)}}{\tilde{H}_e}$$

and

$$\tilde{H}_e = \frac{H_e}{\gamma A(d+z_0)}$$

For given  $L_0/\ell, \beta$  is found from (2.40) and  $\frac{\ell/2}{d}$  from (2.41). If  $\frac{z_0}{\ell/2}$  is

also known, then since  $\frac{\ell/2}{d+z_0} = \frac{\ell/2}{d} \left\{ \frac{1}{1 + \left(\frac{z_0}{\ell/2}\right)\left(\frac{\ell/2}{d}\right)} \right\}$ ,  $\tilde{H}_e$  can be computed

from the expression for  $\beta$ . The limiting condition  $T_{\min} = 0$  occurs when  $\tilde{H}_e = 1$  and for  $\tilde{H}_e < 1$  the cable is in compression over part of its length. Note that the limiting profile is independent of the cross-sectional area of the cable.

The values of  $\frac{L}{\ell}$ ,  $\frac{\ell/2}{d}$ , the angle of the chord to the vertical  $\phi$  and the angle of the upper cable end to the vertical  $\alpha$  (see Fig. 2.9) for the limiting profile are given in Table 2.1 for various values of  $\frac{z_0}{\ell/2}$ . A plot of  $\frac{\ell/2}{d}$  vs.  $\frac{z_0}{d}$  is presented in Fig. 2.9 (where  $\frac{\rho_s}{\rho_w} = \frac{7.85}{1.02} = 7.7$  is used).

The results show that for small values of  $\frac{z_0}{d}$  the critical profiles are very steep and will seldom be realized in practice. However, for large values of  $\frac{z_0}{d}$  the critical profiles are more realistic. Thus for deeply submerged buoys it is possible to have the mooring lines in compression over part of their length.



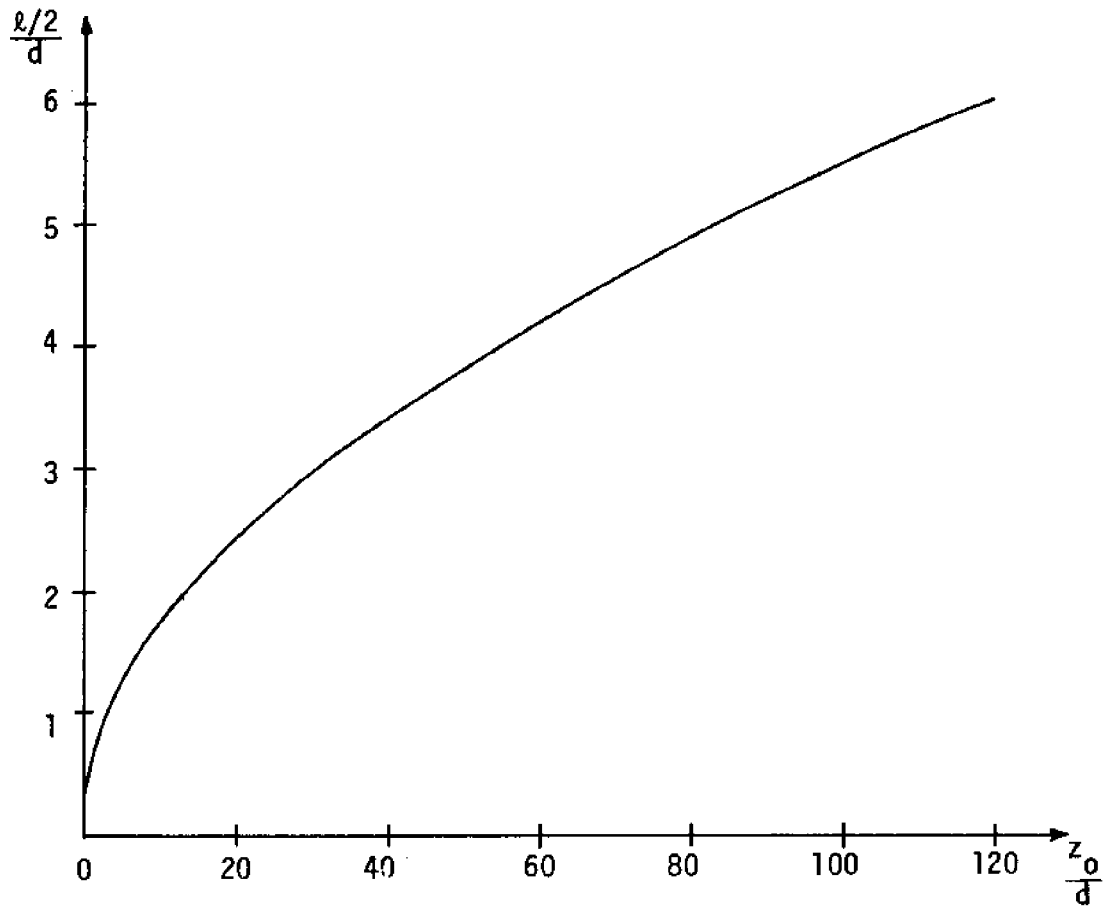


Fig. 2.9 - Plot of  $\frac{l/2}{d}$  vs.  $\frac{z_0}{d}$  for the Limiting Profiles

$\frac{z_0}{\lambda/2}$	$\frac{L}{\lambda}$	$\frac{\lambda/2}{d}$	$\phi$ (degrees)	$\alpha$ (degrees)
0	2.80	0.41	22.1	7.4
1	2.22	0.55	28.7	10.9
2	1.80	0.73	36.2	15.6
3	1.53	0.96	43.8	21.4
4	1.36	1.22	50.6	27.7
6	1.18	1.81	61.1	39.9
8	1.11	2.37	67.1	48.4
10	1.07	3.01	71.6	55.5
15	1.03	4.44	77.3	65.4
20	1.02	6.05	80.6	71.5

Table 2.1: Parameters of the critical profiles for various values of  $\frac{z_0}{\lambda/2}$ .

### CHAPTER 3

#### STATIC ANALYSIS OF SUBMERGED MULTI-LEG CABLE-BUOY SYSTEMS

##### 3.1 Introduction

Various methods exist for the static analysis of a cable-buoy system consisting of a buoy (submerged or surface-moored) attached to the seabed by an array of cables. An accurate analysis that allows for variable current profiles and cable properties can only be performed by using finite element techniques. The aim of this chapter is to develop a simplified, approximate analysis procedure for situations where the cables have constant properties and where the current profile may be assumed to be uniform. The numerical technique derived herein treats whole cables as single elements, and hence requires much less storage requirements than finite element techniques, thereby facilitating the use of micro-computers to obtain approximate solutions.

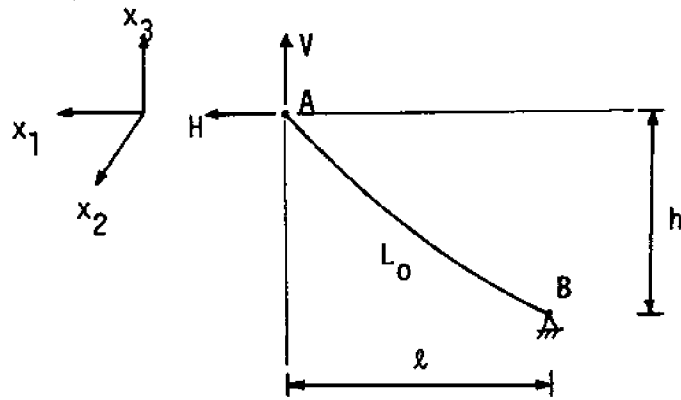
Initially the methodology is developed to analyze the system under a point load applied at the buoy. The approximate treatment of the drag forces induced on the cables by a uniform current profile is then investigated.

##### 3.2 The Tangent Stiffness Matrix for a Cluster of Cables

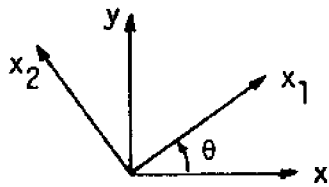
First consider the cable shown in Fig. 3.1(a). Assume that point B is fixed and that the stiffness matrix for small displacements of point A is required. The equations defining the horizontal and vertical forces, H and V, at A implicitly in terms of the cable properties and geometry are (see Section 2.2):

$$l = \frac{HL_0}{EA_0} + \frac{HL_0}{W} \left\{ \sinh^{-1} \left( \frac{V}{H} \right) - \sinh^{-1} \left( \frac{V-W}{H} \right) \right\} \quad (3.1)$$

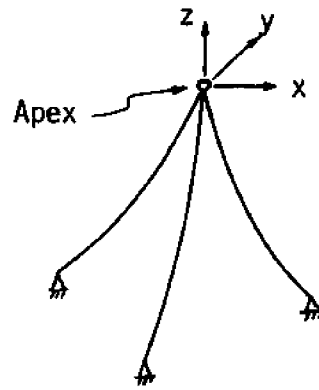
$$h = \frac{WL_0}{EA_0} \left( \frac{V}{W} - \frac{1}{2} \right) + \frac{HL_0}{W} \left[ \left\{ 1 + \left( \frac{V}{H} \right)^2 \right\}^{1/2} - \left\{ 1 + \left( \frac{V-W}{H} \right)^2 \right\}^{1/2} \right] \quad (3.2)$$



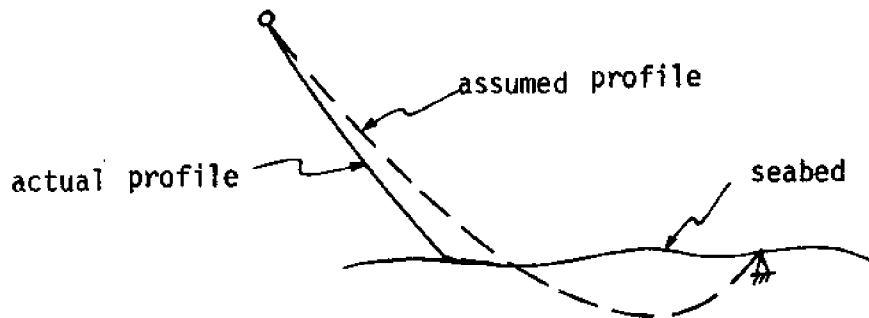
(a) Definition diagram



(b) Local and global coordinate systems



(c) A Typical cable cluster



(d) Approximation when cable lies partially on the seabed

Fig. 3.1 - Illustrations for Derivation of Tangent Stiffness Matrices

The stiffness equation in the  $x_2$  direction is uncoupled from the stiffness equations in the  $x_1$  and  $x_3$  directions. To obtain the stiffnesses in the latter two directions it is easier to first determine the flexibility matrix and then invert it (Irvine, 1981).

Equations (3.1) and (3.2) may be written as

$$\begin{aligned} \ell &= f(H, V) \\ h &= g(H, V) \end{aligned} \quad (3.3)$$

so that

$$\begin{aligned} d\ell &= \frac{\partial f}{\partial H} dH + \frac{\partial f}{\partial V} dV \\ dh &= \frac{\partial g}{\partial H} dH + \frac{\partial g}{\partial V} dV \end{aligned} \quad (3.4)$$

In matrix notation

$$\begin{Bmatrix} d\ell \\ dh \end{Bmatrix} = \underset{\sim}{F} \begin{Bmatrix} dH \\ dV \end{Bmatrix} \quad (3.5)$$

where

$$\underset{\sim}{F} = \begin{bmatrix} \frac{\partial f}{\partial H} & \frac{\partial f}{\partial V} \\ \frac{\partial g}{\partial H} & \frac{\partial g}{\partial V} \end{bmatrix} = \begin{bmatrix} f_{11} & f_{13} \\ f_{31} & f_{33} \end{bmatrix}$$

is the flexibility matrix for displacements in the  $x_1$  and  $x_3$  directions. Evaluating the individual terms

$$f_{11} = \frac{\partial f}{\partial H} = \frac{L_0}{EA_0} + \frac{L_0}{W} \left[ \sinh^{-1} \left( \frac{V}{H} \right) - \sinh^{-1} \left( \frac{V-W}{H} \right) - \frac{V/H}{\left\{ 1 + (V/H)^2 \right\}^{1/2}} + \frac{(V-W)/H}{\left\{ 1 + ((V-W)/H)^2 \right\}^{1/2}} \right] \quad (3.6)$$

$$f_{13} = \frac{\partial f}{\partial V} = \frac{L_0}{W} \left[ \left\{ 1 + \left( \frac{V}{H} \right)^2 \right\}^{-1/2} - \left\{ 1 + \left( \frac{V-W}{H} \right)^2 \right\}^{-1/2} \right] \quad (3.7)$$

$$f_{31} = \frac{\partial g}{\partial H} = \frac{L_0}{W} \left[ \left\{ 1 + \left( \frac{V}{H} \right)^2 \right\}^{1/2} - \left\{ 1 + \left( \frac{V-W}{H} \right)^2 \right\}^{1/2} - \frac{(V/H)^2}{\left\{ 1 + (V/H)^2 \right\}^{1/2}} + \frac{((V-W)/H)^2}{\left\{ 1 + ((V-W)/H)^2 \right\}^{1/2}} \right] \quad (3.8)$$

$$f_{33} = \frac{\partial g}{\partial V} = \frac{L_0}{EA_0} + \frac{L_0}{W} \left[ \frac{V/H}{\left\{ 1 + (V/H)^2 \right\}^{1/2}} - \frac{(V-W)/H}{\left\{ 1 + ((V-W)/H)^2 \right\}^{1/2}} \right] \quad (3.9)$$

(For purposes of calculation it is best to replace the inverse hyperbolic sine by its logarithmic representation, namely,  $\sinh^{-1} x = \ln \{ x + (1+x^2)^{1/2} \}$  ).

The stiffness matrix is the inverse of the flexibility matrix. Thus

$$\tilde{K}' = \frac{1}{\det \tilde{F}} \begin{bmatrix} f_{33} & -f_{13} \\ -f_{31} & f_{11} \end{bmatrix} = \begin{bmatrix} k_{11} & k_{13} \\ k_{31} & k_{33} \end{bmatrix} \quad (3.10)$$

In the  $x_2$  direction the stiffness of small displacements is simply  $k_{22} = H/\ell$ . Thus the complete tangent stiffness matrix at A is

$$\tilde{K} = \begin{bmatrix} k_{11} & 0 & k_{13} \\ 0 & k_{22} & 0 \\ k_{31} & 0 & k_{33} \end{bmatrix} \quad (3.11)$$

Now consider the coordinate axes shown in Fig. 3.1(b). The local coordinate system is  $(x_1, x_2, x_3)$ , while the global coordinate system is  $(x, y, z)$ , where the  $x_3$  and  $z$  axes are taken to be identical. The transformation from local  $\tilde{x}_\ell$  to global  $\tilde{x}_g$  coordinates may be described by a transformation matrix  $R$  defined by

$$\tilde{x}_\ell = R \tilde{x}_g$$

or

$$\text{or } \begin{Bmatrix} x_1 \\ x_2 \\ x_3 \end{Bmatrix} = \begin{bmatrix} \cos \theta & \sin \theta & 0 \\ -\sin \theta & \cos \theta & 0 \\ 0 & 0 & 1 \end{bmatrix} \begin{Bmatrix} x \\ y \\ z \end{Bmatrix} \quad (3.12)$$

$$\text{Since } \begin{aligned} \tilde{R}^{-1} &= \tilde{R}^T, \\ \tilde{x}_g &= \tilde{R}^T \tilde{x}_l \end{aligned}$$

If the tangent stiffness matrix for the cable is  $\tilde{K}_l$  in the local system and  $\tilde{K}_g$  in the global system, then

$$\begin{aligned} \tilde{K}_g &= \tilde{R}^T \tilde{K}_l \tilde{R} \\ &= \begin{bmatrix} k_{11} \cos^2 \theta + k_{22} \sin^2 \theta & (k_{11} - k_{22}) \sin \theta \cos \theta & k_{13} \cos \theta \\ (k_{11} - k_{22}) \sin \theta \cos \theta & k_{11} \sin^2 \theta + k_{22} \cos^2 \theta & k_{13} \sin \theta \\ k_{31} \cos \theta & k_{31} \sin \theta & k_{33} \end{bmatrix} \end{aligned} \quad (3.13)$$

where  $k_{11}$ ,  $k_{13}$  etc. are as defined in (3.11). Note that in general the tangent stiffness matrix is not symmetric.

For a cluster of cables meeting at a point (see Fig. 3.1(c)) the global tangent stiffness matrix for small displacements of the common apex may be obtained by determining the global stiffness matrix (through the local stiffness matrix) for each cable, and then summing all of these matrices.

For cases such as surface-moored buoys, where the displacement of the apex is constrained in the  $z$  (or  $x_3$ ) direction, the  $2 \times 2$  tangent stiffness matrix corresponding to displacements in the  $x$  and  $y$  directions consists of the first two rows and columns of the  $3 \times 3$  matrix of (3.13).

### 3.3 Static Analysis Using a Tangent Stiffness Solution Procedure

The problem to be analyzed here is that of a submerged cable-buoy system acted on by a point load at the buoy. This system exhibits a stiffening type of nonlinear behavior. That is, the increment in displacement for constant increments of applied load becomes successively smaller as the buoy displaces from its initial equilibrium state. It is assumed that the cables remain elastic and hence the nonlinearity is solely geometric. There are various iterative and incremental solution techniques that may be used to solve such a problem.

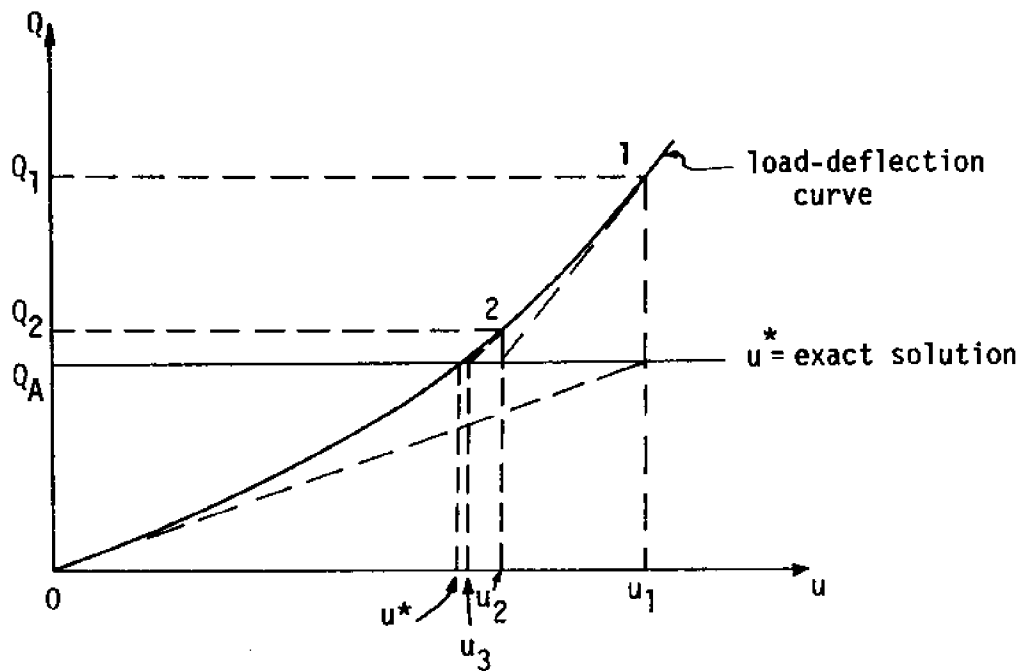
The method used here is an iterative procedure that utilizes the tangent stiffness matrix of the cable cluster, and is similar to the well-known Newton-Raphson method for the solution of nonlinear equations.

A procedure by which the tangent stiffness matrix of a cable cluster can be computed was outlined in the previous section. This was based on the assumption that the cable profiles were catenaries. The profiles of submerged cables are catenaries only if they are either inextensible or incompressible (as shown in Chapter 2), and since the tangent stiffness matrix of the submerged cable cluster is required in the analysis technique developed herein it is assumed that the cables meet one of these requirements. The weight  $W$  used in the previous section is thus the effective weight,  $(mg - \gamma A_0)L_0$ , and the forces  $H$  and  $V$  are the effective forces corresponding to the effective tension at the upper end of the cable (see Section 2.3).

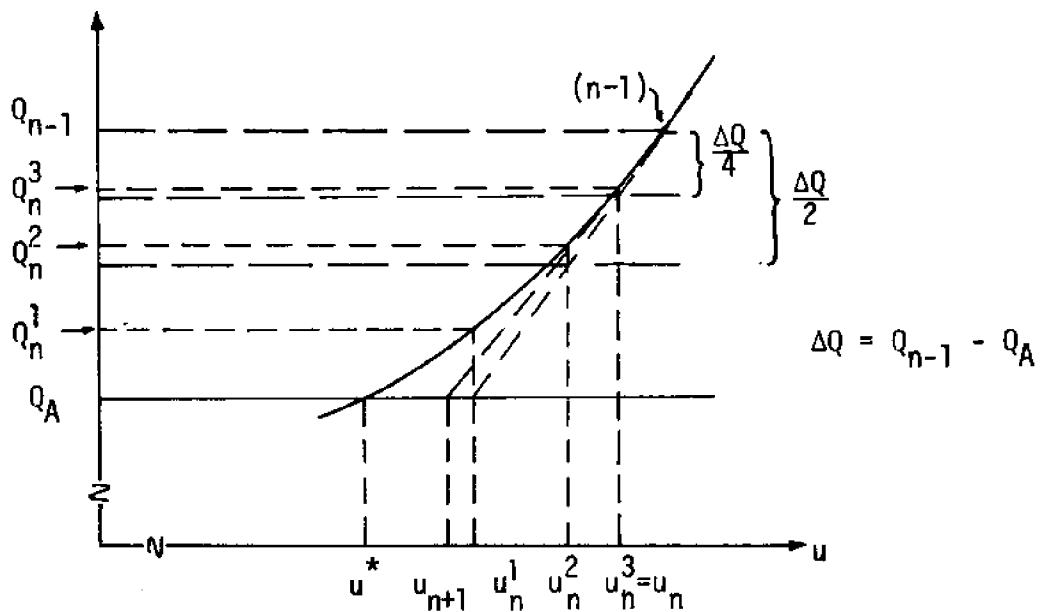
The possibility of a long cable lying on the seabed for part of its length is also neglected in determining the tangent stiffness matrix and the end forces of that cable. Fig. 3.1(d) shows the profile assumed in computing the stiffness and end forces of such a cable. The slight discrepancy in the stiffness matrix is not critical since it alters only the "path" to the solution. The discrepancy in end forces when checking equilibrium at the final displacement is of more importance, but this difference is not expected to be too significant.

Fig. 3.2(a) shows a one-dimensional representation of the solution technique. The applied load is  $Q_A$  and the first estimate of the deflec-





(a) Tangent stiffness solution procedure



(b) Strategy used when convergence is not obtained

Fig. 3.2 - One-Dimensional Representations of Solution Technique

tion,  $u_1$ , is found by using the initial tangent stiffness. The load  $Q_1$  required to maintain the system at equilibrium is then computed. The tangent stiffness at point 1 is used with the unbalanced load ( $Q_A - Q_1$ ) to obtain the improved estimate of the deflection  $u_2$ . The iteration is continued until the  $n^{\text{th}}$  estimate  $u_n$  is such that the unbalanced load ( $Q_A - Q_n$ ) and the increment in displacement ( $u_n - u_{n-1}$ ) are sufficiently small.

The problem to be solved is a three-dimensional one, but the solution procedure is essentially the same. The loads  $Q$  and displacements  $u$  are in this case vector quantities and the tangent stiffness is represented by a 3 x 3 matrix  $K$ . The iteration may be expressed as

$$\underline{u}_n = \underline{u}_{n-1} + \underline{K}_{n-1}^{-1} (\underline{Q}_A - \underline{Q}_{n-1}) \quad (3.14)$$

where  $Q_A$  is the applied load,  $u_n$  the  $n^{\text{th}}$  estimate of the displacement,  $Q_{n-1}$  is the load that is required to maintain the system at equilibrium at the displacement  $u_{n-1}$ , and  $K_{n-1}$  is the tangent stiffness matrix at  $u_{n-1}$ . A suitable check for convergence is

$$\frac{|\underline{u}_n - \underline{u}_{n-1}|}{|\underline{u}_n|} < \epsilon_1 \quad \text{and} \quad \frac{|\underline{Q}_A - \underline{Q}_n|}{|\underline{Q}_A|} < \epsilon_2 \quad (3.15)$$

where  $||$  represents the magnitude of the enclosed vectors and  $\epsilon_1, \epsilon_2$  are specified error limits.

The computation of  $Q_n$  requires the horizontal and vertical effective forces  $H$  and  $V$  in local coordinates (see Fig. 3.1(a)) to be calculated for each cable in the cluster, when the common apex is located at  $u_n$ . The values of  $H$  and  $V$  are also required to compute  $K_n$ . To find these forces the two nonlinear simultaneous equations (3.1) and (3.2) need to be solved. In general, this needs to be done numerically and a two-dimensional Newton-Raphson scheme is one possible technique. Writing (3.1) and (3.2) as

$$\begin{aligned} F(H,V) &= f(H,V) - \ell \\ G(H,V) &= g(H,V) - h \end{aligned} \quad (3.16)$$

The Newton-Raphson iterative scheme may be expressed as

$$\begin{Bmatrix} H \\ V \end{Bmatrix}_n = \begin{Bmatrix} H \\ V \end{Bmatrix}_{n-1} + \begin{Bmatrix} \Delta H \\ \Delta V \end{Bmatrix}_{n-1} \quad (3.17)$$

with

$$\Delta H_{n-1} = \frac{G F_V - F G_V}{F_H G_V - F_V G_H}$$

$$\Delta V_{n-1} = \frac{F G_H - G F_H}{F_H G_V - F_V G_H}$$

where  $F_H = \frac{\partial F}{\partial H} = \frac{\partial f}{\partial H}$  etc. (same as (3.6) to (3.9)) and each of the functions are evaluated at  $(H_{n-1}, V_{n-1})$ . A suitable convergence criterion is

$$\left\{ \frac{(\Delta H_{n-1})^2 + (\Delta V_{n-1})^2}{H_n^2 + V_n^2} \right\}^{1/2} < \epsilon \quad (3.18)$$

Thus for each step of the tangent stiffness solution procedure, a Newton-Raphson iteration is required to compute H and V. One drawback with the latter technique is that fairly good initial guesses of H and V are required for convergence. This problem can be overcome by using the following strategy. At the  $n^{\text{th}}$  step of the tangent stiffness procedure, the values of H and V obtained at the  $(n-1)^{\text{th}}$  step are used as initial guesses. If the Newton-Raphson procedure diverges or does not converge within a specified number of iterations, then the increment in load from the  $(n-1)^{\text{th}}$  step to the  $n^{\text{th}}$  step,  $(Q_A - Q_{n-1})$ , is halved,  $u_n$  is recomputed and calculation of H and V is attempted. This can be repeated as many times as is necessary to obtain H and V at some displacement  $|u_n| > |u_{n-1}|$ . Fig. 3.2(b) shows a one-dimensional representation of a hypothetical case. From the point  $(n-1)$  the value of  $u_n^1$  is obtained, but  $Q_n^1$  could not be obtained because the Newton-Raphson iteration to compute H and V for one of the cables in the cluster did not converge.

Then the load increment is halved and  $u_n^2$  computed. Again the Newton-Raphson iteration failed for a cable and hence  $Q_n^2$  could not be found. The load increment is halved again and  $u_n^3$  calculated where the Newton-Raphson scheme converged and  $Q_n^3$  was able to be found. The value of  $u_{n+1}$  is then obtained from  $u_n^3$ ,  $Q_n^3$  and the tangent stiffness at  $u_n^3$ .

When starting the problem, an initial position needs to be prescribed for the buoy. If the initial equilibrium position of the buoy (i.e., when no lateral loads are acting) is known, then this may be used, but any other position is equally valid. If the end forces in the cables are unknown at this configuration, then initial guesses need to be supplied and the correct values of these forces determined by solving equations (3.1) and (3.2) before the tangent stiffness iteration procedure can be commenced. It has been found that overestimates of the horizontal and vertical forces (H and V) at a cable end sometimes results in divergence or poor convergence. When the prescribed initial position of the buoy is roughly in the center of the area defined by the anchor points of the cables on the seabed, initial guesses of  $V = 0.5W$  and  $H = 0.1W$  to  $0.2W$  have been often found to lead to convergent solutions (where  $W$  is the total effective weight of the corresponding cable). Note that the initial equilibrium position of the buoy can also be found, if required, by specifying the buoyancy force on the buoy as the only applied load.

#### 3.4 Approximate Treatment of a Uniform Current Profile for Flat-Sag Cables

The presence of drag forces on the cables due to sea currents add complexity to the problem and in general the analysis requires a finite element solution technique. An approximate solution is presented here for the special case when the current velocity profile is invariant with depth and when the sags in the cables are small. The aim is to obtain equivalent loads that are to be applied to the buoy due to drag forces on the cables.

Consider a cable segment located in a velocity field as shown in Fig. 3.3. The drag forces per unit length of the segment are due to the normal (in-plane and out-of-plane) and tangential velocity components with magnitudes given by (Berteaux, 1976):

$$\begin{aligned}
 F_{NI} &= \frac{1}{2} \rho C_n d (V \cos \theta \sin \phi)^2 && \text{(in-plane)} \\
 F_{NO} &= \frac{1}{2} \rho C_n d (V \sin \theta)^2 && \text{(out-of-plane)} \\
 F_T &= \frac{1}{2} \rho C_f \pi d (V \cos \theta \cos \phi)^2
 \end{aligned} \tag{3.19}$$

where  $\rho$  is the density of the water,  $C_n$  and  $C_f$  are the normal and tangential drag coefficients,  $d$  is the diameter of the cable,  $V$  is the current velocity, and  $\theta$  and  $\phi$  are the plan and elevation angles between the cable axis and the current direction. For most cables  $C_f \ll C_n$  (i.e.  $C_f \approx 0$ ) and the tangential drag force may be neglected.

For a flat-sag cable, an approximate expression for the profile can be found with the assumption that the weight of the cable is uniformly distributed along the chord connecting the cable ends. It is convenient to use inclined coordinates  $x$  and  $y$  as shown in Fig. 3.4.

First consider the profile of the cable under self-weight alone. Equilibrium of forces in the  $y$ -direction yields

$$H(x) \frac{dy}{dx} = w \left( \frac{\ell}{2} - x \right) \cos \beta \tag{3.20}$$

where  $H(x)$  is the  $x$ -component of cable tension,  $\ell$  is the chord length,  $\beta$  is the inclination of the chord to the horizontal, and  $w$  the effective weight of the cable. Equilibrium in the  $x$  direction gives

$$H(x) = H + w x \sin \beta \tag{3.21}$$

where  $H = H(\ell)$ .

The cable behaves approximately like a taut string to the out-of-plane normal load on it. Thus approximately half the total load will be transferred to each end. The out-of-plane deflection of the cable will be neglected here. The in-plane normal load is nonuniform and varies in direction over the length of the cable. However, a reasonable approximation is to assume that it is uniformly distributed over the chord length and is normal to  $H$ . The additional deflection due to the in-plane normal load  $p$  is denoted by  $v$ . The increase in  $H(x)$  due to  $p$  is a constant,  $h$ ,

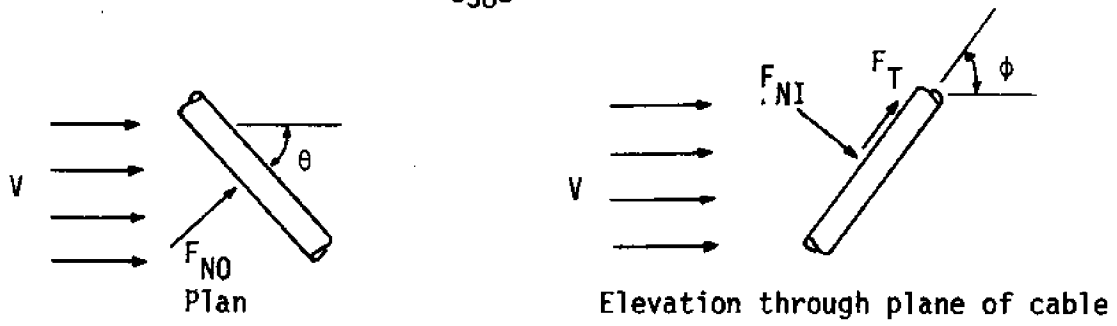


Fig. 3.3 - Drag Forces on a Cable Element

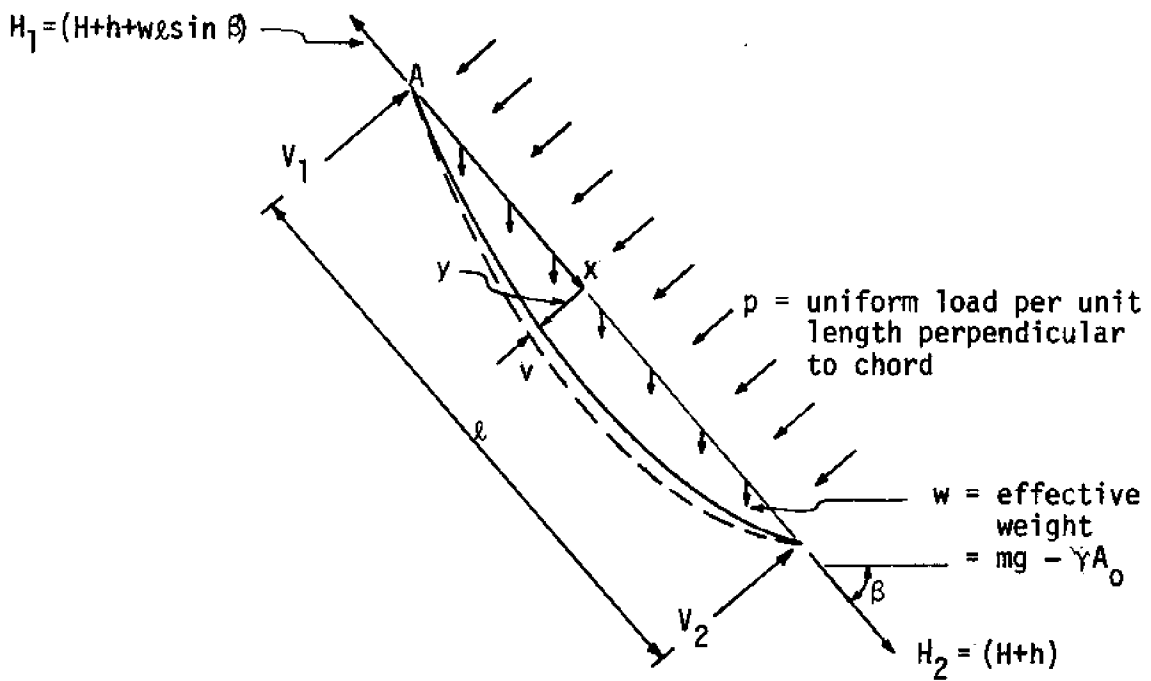


Fig. 3.4 - In-plane Loading on an Inclined Flat-sag Cable

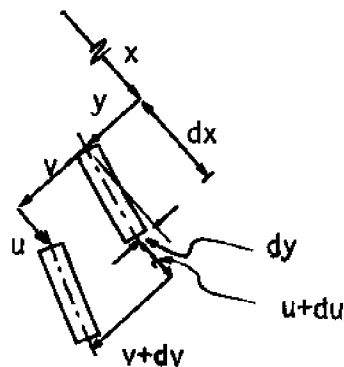


Fig. 3.5 - Displacements of an Element of the Cable

since the additional load is applied only in the y-direction. Equilibrium of forces in the y-direction now yields

$$(H(x) + h) \frac{d}{dx} (y+v) = w\left(\frac{l}{2} - x\right) \cos \beta + p\left(\frac{l}{2} - x\right) \quad (3.21)$$

Using (3.20), (3.21) and neglecting the second-order term

$$\frac{dv}{dx} = \frac{p\left(\frac{l}{2} - x\right)}{H + wx \sin \beta} - \frac{hw\left(\frac{l}{2} - x\right) \cos \beta}{(H + wx \sin \beta)^2} \quad (3.22)$$

To complete the solution, h must be evaluated. This is done by using a cable equation that incorporates the cable elasticity to provide a closure condition relating the changes in cable tension to the changes in cable geometry. The displacement of an element of the cable is shown in Fig. 3.5. If ds is the original length of the element and ds' is its new length, then

$$ds^2 = dx^2 + dy^2 \quad (3.23)$$

$$ds'^2 = (dx + du)^2 + (dy + dv)^2$$

where u and v are the x and y components of the displacements, respectively. For the flat-sag cable the fractional change in length, correct to the second order of small quantities, is

$$\frac{ds' - ds}{ds} = \frac{du}{ds} \frac{dx}{ds} + \frac{dv}{ds} \frac{dy}{ds} + \frac{1}{2} \left(\frac{dv}{ds}\right)^2 \quad (3.24)$$

The desired form of Hooke's law for the incompressible cable, with  $\tau$  denoting the increase in effective tension and not the increase in actual tension in the cable, is (from (2.34))

$$\frac{\tau}{EA_0} = \frac{ds' - ds}{ds} \quad (3.25)$$

But, to second order,  $\tau = h \frac{ds}{dx}$ , so that the cable equation for the element becomes

$$\frac{h(ds/dx)^3}{EA_0} = \frac{du}{dx} + \frac{dy}{dx} \frac{dv}{dx} + \frac{1}{2} \left(\frac{dv}{dx}\right)^2 \quad (3.26)$$

It is convenient to use the cable equation in the integrated form

$$\frac{hL_e}{EA_0} = \int_0^{\ell} \frac{dy}{dx} \frac{dv}{dx} dx + \frac{1}{2} \int_0^{\ell} \left(\frac{dv}{dx}\right)^2 dx \quad (3.27)$$

where  $L_e = \int_0^{\ell} \left(\frac{ds}{dx}\right)^3 dx$  is a quantity only a little greater than the chord length  $\ell$ .

Although the two terms on the right-hand side of (3.27) can be evaluated using (3.20), (3.21) and (3.22), little error is introduced by using the linearized version of (3.27) (i.e., neglecting the last term) when the in-plane normal drag forces are small compared to the existing forces (i.e., self-weight and initial tension).

Substituting for  $\frac{dy}{dx}$  and  $\frac{dv}{dx}$  from (3.20) and (3.22) and performing the required integration in the linearized cable equation, the required quantity  $h$  can be determined from

$$\frac{h}{H} = \frac{\left(\frac{P\ell}{H}\right) C \tan \beta}{\left(\frac{wL_e}{EA_0}\right) \tan^2 \beta \sin \beta + D} \quad (3.28)$$

where

$$C = 2 + \frac{1}{4\gamma(\gamma+1)} - (2\gamma+1) \ln\left(1 + \frac{1}{\gamma}\right)$$

$$D = \ln\left(1 + \frac{1}{\gamma}\right) - \frac{1}{8} \left(\frac{2\gamma+1}{\gamma^2}\right) \frac{(4\gamma^2 + 4\gamma - 1)}{(\gamma+1)^2}$$

$$\gamma = \frac{H}{w \ell \sin \beta}$$

Equation (3.28) is arranged in nondimensional form for convenience. In determining  $h$  the value of  $L_e$  may be approximated by  $\ell$ .

The in-plane loads applied on a buoy attached to the upper end of the flat-sag cable in a uniform current is thus  $H_1 (= H + h + w \ell \sin \beta)$



and  $V_1$ , with directions that are opposite to the reactions at point A in Fig. 3.4. The values of  $H$  and  $V_1$  may be estimated as described subsequently. Once  $H$  is known,  $h$  can be obtained from (3.28) and thus the in-plane forces at A can be determined.

Consider the cable shown in Fig. 3.6 loaded with an effective weight  $w$ . The profile of the cable is a catenary (incompressible cable) and the effective forces  $H'$  and  $V'$  can be determined by solving simultaneously the equations analogous to (3.1) and (3.2). The force components in the  $x$  and  $y$  directions are

$$\begin{aligned} H'' &= H' \cos \beta + V' \sin \beta \\ V'' &= -H' \sin \beta + V' \cos \beta \end{aligned} \quad (3.29)$$

$H$  is the  $x$ -component of the reaction at B and is thus given by

$$H = H'' - w \ell \sin \beta \quad (3.30)$$

When a uniform load of intensity  $p$  per unit length is applied normal to the chord in the negative  $y$ -direction, the reaction in the  $y$ -direction at A is

$$V_1 = V'' + \frac{p\ell}{2} \quad (3.31)$$

Note that  $p$  is the same as  $F_{NI}$  of (3.19).

Also note that for the typical cable cluster shown in Fig. 3.7 the in-plane normal drag on the cables causes an increase in tension in cables 1 and 2, but a decrease in tension in cable 3. The resultant of all the equivalent loads at the buoy due to the in-plane and out-of-plane drag forces on the cables, together with the buoyancy and drag forces on the buoy, should be in equilibrium at the final displaced position of the buoy.

The technique described in Section 3.3 may be adopted to obtain a solution for this case. However, the tangent stiffness matrix of each cable (and hence the cluster) is not easy to evaluate. Although the forces at point A in the cable of Fig. 3.4 are dependent only on  $\ell$  and  $\beta$ , the two equations for  $H_1$  and  $V_1$  are implicit (i.e.,  $f(H_1, V_1, \ell, \beta) = 0$ ,

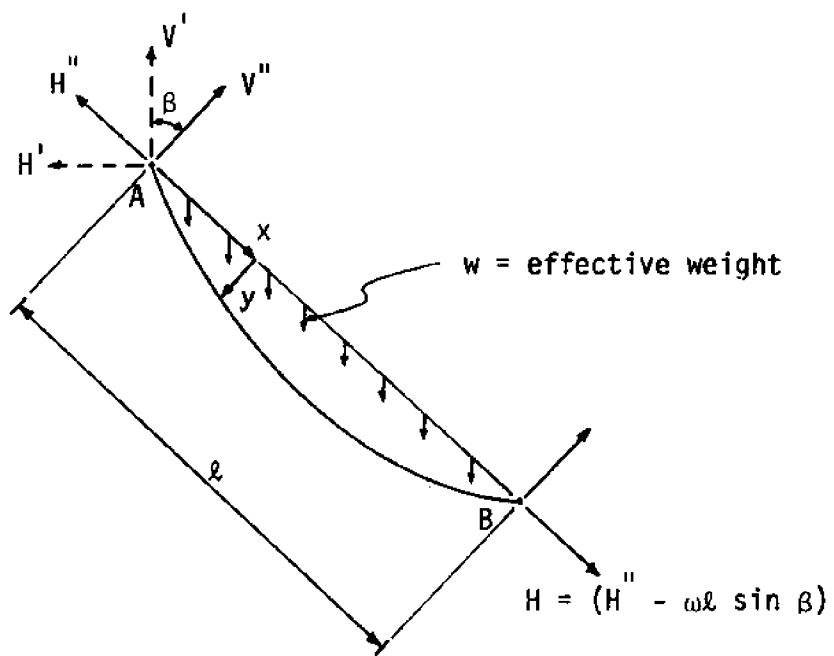


Fig. 3.6 - End Forces Due to Self Weight Only

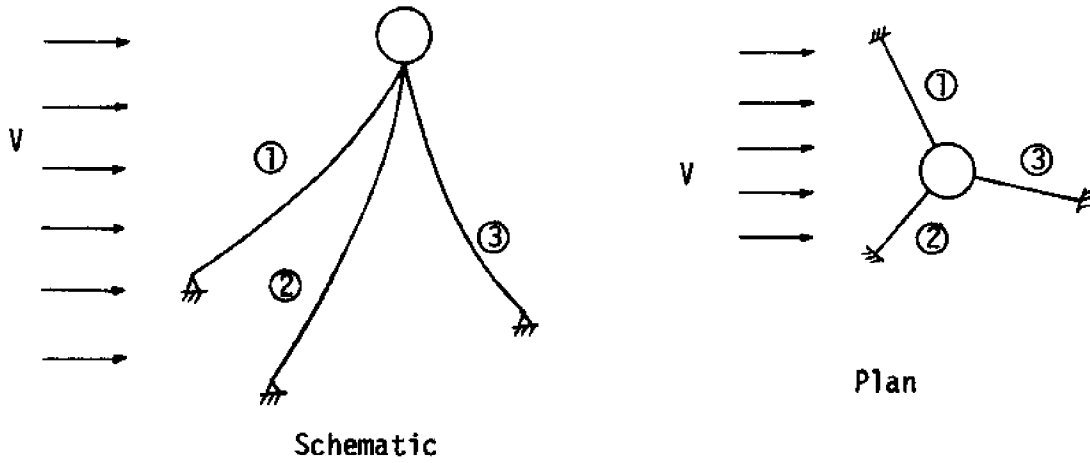


Fig. 3.7 - A Typical Cable Cluster

$g(H_1, V_1, \ell, \beta) = 0$ ), which makes the extraction of a tangent stiffness or flexibility matrix difficult.

An alternative, ad hoc, way of proceeding is to apply loads at the buoy to account for the current drag on the cables and then proceed with the analysis as if no currents are present. This will give an estimate of the required solutions. The loads applied at the buoy due to the effective weight of a single cable are  $H''$  and  $V''$  (see Fig. 3.6) computed from (3.29). The in-plane loads due to the effective weight and the in-plane current drag are  $H_1$  and  $V_1$  (see Fig. 3.4). Thus the in-plane loads to be applied at the buoy due to current drag alone are  $h(=H_1 - H'')$  and  $\frac{p\ell}{2}(=V_1 - V'')$ . Note that in this case it is best to first compute the equilibrium position of the buoy when no current is acting, and use this configuration to estimate the equivalent forces on the buoy due to current drag on the cables.

#### Summary of Approximate Analysis under Uniform Current

The approximate analysis technique described in this section is summarized here in sequential steps. Note that in all calculations the effective weight of the cables should be used.

##### I. Obtain solution with no current forces.

- (1) Decide on an initial position for the buoy and guess the horizontal and vertical in-plane effective forces at the upper end of each cable. Solve equations (3.1) and (3.2) using these initial guesses and the Newton-Raphson scheme described in Section 3.2 to obtain accurate values of these horizontal and vertical effective forces.
- (2) Specifying the applied force at the buoy  $Q_A$  equal to the vertical buoyancy force on the buoy, find the equilibrium position of the buoy when no lateral loads are acting by using the tangent stiffness procedure described in Section 3.3. Note that the initial unbalanced load is  $Q_A - Q$ , where  $Q$  is the resultant of the horizontal and vertical cable forces computed in (1) above. Also compute the horizontal and vertical effective forces  $H'$  and  $V'$  in each cable in the equilibrium position.

II. Obtain solution when current loads are acting.

- (1) Using the quantities  $H'$  and  $V'$  for the cables in the equilibrium position without current loads, compute for each cable
  - (i)  $H''$  and  $V''$  from (3.29)
  - (ii)  $H$  and  $V_1$  from (3.30) and (3.31)
  - (iii)  $h$  using (3.28) and  $H_1 = H + h + w \ell \sin \beta$
  - (iv)  $H_I^* = H_1 - H'' = h$  and  $V_I^* = V_1 - V'' = \frac{p\ell}{2}$
  - (v) out-of-plane forces  $H_O^*$  which is half the total out-of-plane drag force on the cable.
- (2) Add vectorially the contributions  $-H_I^*$ ,  $-V_I^*$  and  $-H_O^*$  from all cables together with the buoyancy and drag forces on the buoy to obtain the resultant applied force  $\underline{Q}_A$ .
- (3) Now that the drag forces are included into  $\underline{Q}_A$ , the resisting forces in each cable are the horizontal and vertical forces  $H'$  and  $V'$  calculated in I(2) above. The resultant of these is  $\underline{Q}$ .
- (4) Use the tangent stiffness technique described in Section 3.3 with  $\underline{Q}_A - \underline{Q}$  as the initial unbalanced load to compute the approximate static displacement of the buoy.
- (5) The effective tensions in the cables at the displaced position can be estimated from (2.15) and from this estimates of the real cable tensions can be obtained using (2.29).

3.5 Example - A Tri-moored Subsurface Buoy

The static analysis of a tri-moored subsurface buoy is presented here to exemplify the analysis procedure described in the previous sections. The plan view of Fig. 3.8 shows the position of the anchor points. The required data is given below.

Data

- 1) Coordinates of anchor points:
 

Point 1	=	(-100, 0, -705) m
Point 2	=	(50, 86.6, -702) m
Point 3	=	(50, -86.6, -700) m

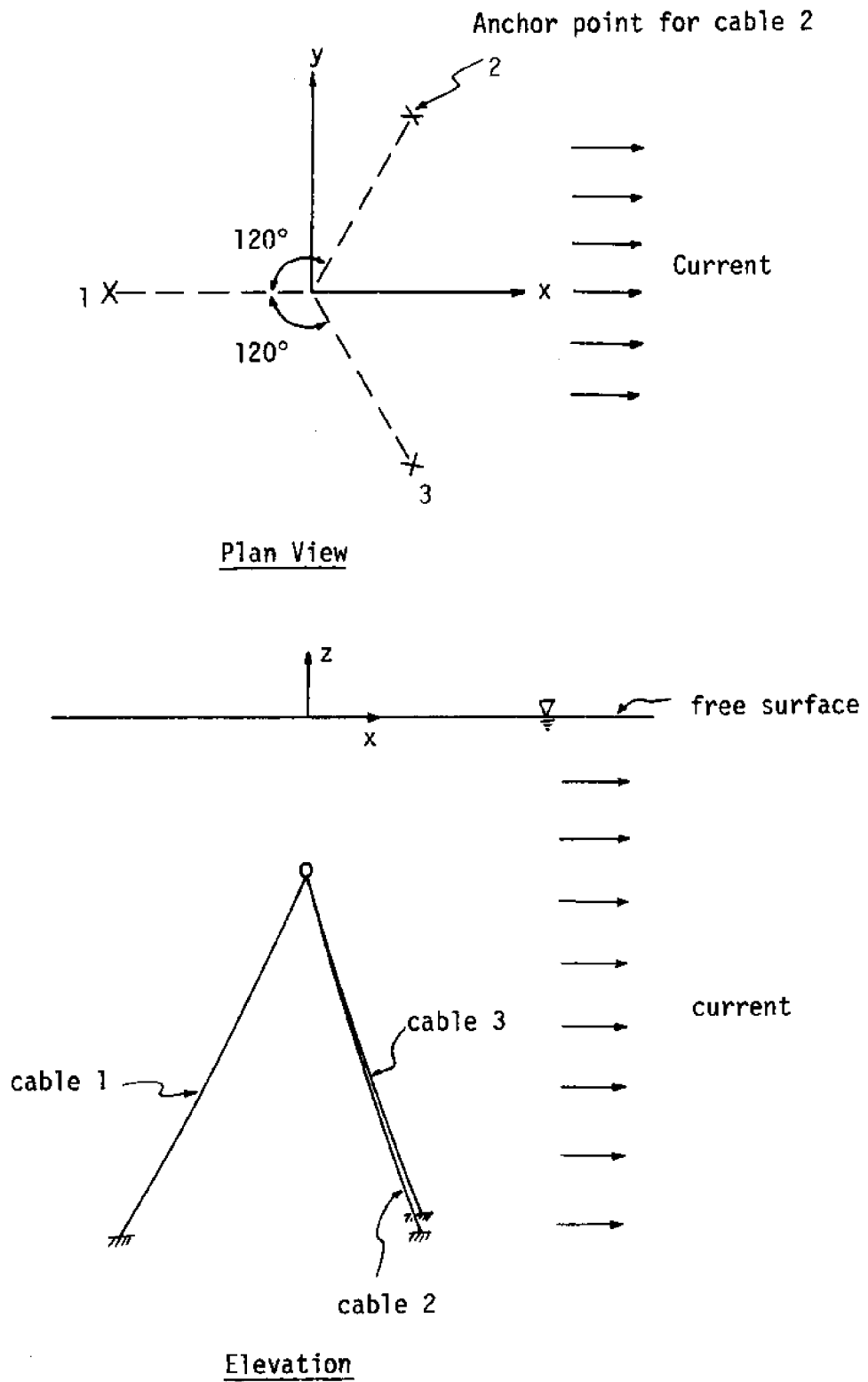


Fig. 3.8 - Definition Diagram for Numerical Example

2) All cables are identical having the following properties:

Diameter	= 12.7 mm ( $\frac{1}{2}$ " )
Youngs' modulus, E	= $172.4(10)^9$ Pa
Length, $L_0$	= 500 m
Density	= $7850 \text{ kg/m}^3$
Normal drag coefficient, $C_n$	= 0.7

3) Properties of the spherical buoy are:

Outer diameter	= 3.0 m
Weight	= 43 kN (i.e., 20 mm thick steel shell)
Drag coefficient, $C_n$	= 0.7

4. A current of 1 m/s (2 knots) is acting in the positive x-direction.

5) z-ordinate of free surface = 300 m.

Acceleration under gravity,  $g = 9.81 \text{ m/s}^2$

Density of sea water =  $1020 \text{ kg/m}^3$ .

#### Applied load on buoy

Net upward force	= weight of water displaced by buoy - weight of buoy
	= 95.7 kN
Drag force	= 2.5 kN
∴ Applied force	= (2500, 0, 95700) N

Solutions

(a) Null current (i.e., no drag forces)

Initial guess for position of buoy = (0, 0, -300).

With the only applied load being a vertical upward force of 95.7 kN, the equilibrium position of the buoy = (-12.18, 5.23, -211.94) m.

Maximum stresses in the cables (under the actual tensions and not the equivalent tensions) in the equilibrium configuration are:

Cable 1 - 314 MPa  
Cable 2 - 249 MPa  
Cable 3 - 206 MPa

(Note: 414 MPa = 60 ksi).

(b) Drag forces on buoy only

Neglecting the drag forces on the cables, the equilibrium position of the buoy = (-11.23, 5.21, -211.93) m.

Maximum stresses in the cables in the equilibrium configuration are:

Cable 1 - 375 Mpa  
Cable 2 - 218 Mpa  
Cable 3 - 175 MPa.

(c) Drag forces on buoy and cables.

Using the approximate treatment presented in Section 3.4, the equivalent loads to be applied at the buoy due to current drag on the cables are:

Cable 1 - (0.7, 0.0, -2.6) kN  
Cable 2 - (0.6, -0.4, 1.7) kN  
Cable 3 - (0.6, 0.5, 2.1) kN

Together with these forces and the drag force on the buoy, the equilibrium position of the buoy = (-10.53, 5.26, -211.91) m.

Maximum stresses in the cables in the equilibrium configuration are:

Cable 1 - 424 MPa

Cable 2 - 194 MPa

Cable 3 - 160 MPa

### Comments

The results show that the excursion of the buoy due to the current is small. This is to be expected, since the net upward force on the buoy is much larger than the lateral drag forces. Buoys submerged to greater depths will be heavier (since they will have to withstand greater pressures) and subsequently the ratio of horizontal to vertical loads on them will be larger, resulting in greater excursions.

The effect of the drag forces on the cables is quite significant. The horizontal displacement of the buoy and the increase in the maximum stress in cable 1 due to drag on the cables are about 3/4 of the corresponding quantities due to drag on the buoy alone.

Note that under the current load, the stresses in cables 2 and 3 are reduced from their initial values, while the stress in cable 1 is increased. The stress in cable 1 only slightly exceeds 60 ksi, which is a reasonable value for the maximum allowable stress.



## CHAPTER 4

### APPLICATION OF STATIC ANALYSIS PROCEDURE TO OTHER CABLE SYSTEMS

The tangent stiffness solution technique developed in Chapter 3 can be applied to more complex cable systems with a larger number of degrees of freedom. The two particular cases considered here are multi-buoy systems and moored semisubmersibles.

#### 4.1 Multi-buoy Systems

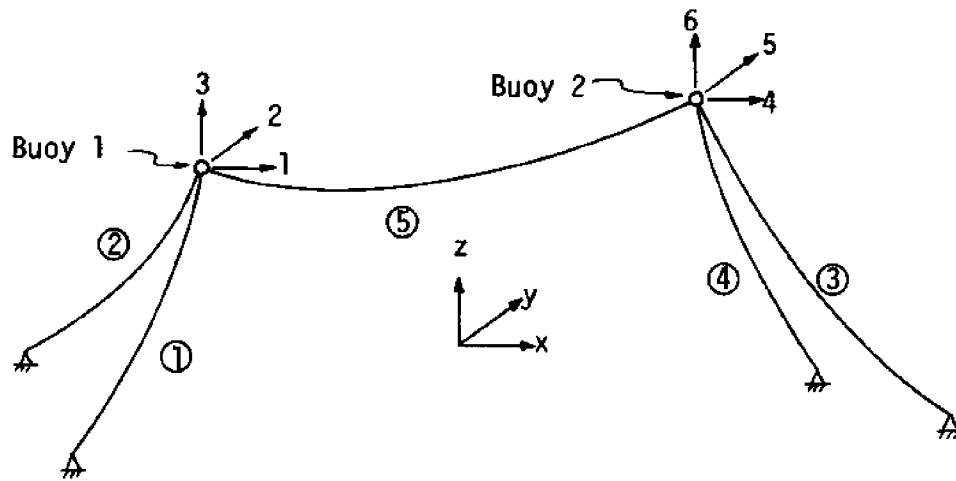
For submerged or surface-moored multi-buoy systems the extension of the analysis procedure developed in Chapter 3 is quite straightforward. Every additional buoy in a system proportionally increases the number of degrees of freedom and hence the size of the tangent stiffness matrix of the system. The analysis procedure remains essentially the same.

As an example consider the two-buoy system shown in Fig. 4.1(a). In general the system has six degrees of freedom corresponding to the x, y and z displacements of each buoy. The tangent stiffness matrices for cables 1 and 2, for small displacements of buoy 1 in the x, y and z directions, can be computed as described in Chapter 3 (i.e. by first computing the stiffnesses in local coordinates and then performing the necessary coordinate transformations). Similarly the stiffness matrices for cables 3 and 4 for small displacements of buoy 2 can also be determined. Let these 3 x 3 stiffness matrices be denoted by  $\tilde{K}^i$ ,  $i = 1, 2, 3, 4$ . Cable 5 has to be treated differently because it results in coupling between the two buoys.

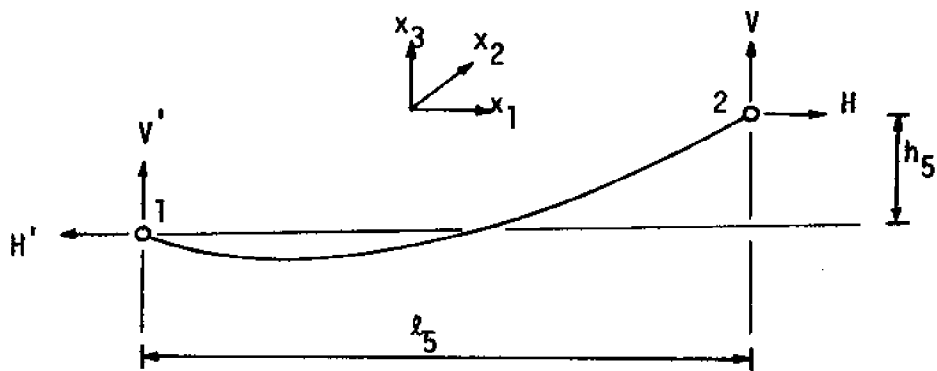
Fig. 4.1(b) shows an in-plane elevation of cable 5 and the equilibrating end forces on it. As before, the two equations that relate the dimensions  $l_5$  and  $h_5$  to the end forces at the higher end H and V are of the form

$$\begin{aligned} l_5 &= f(H, V) \\ h_5 &= g(H, V) \end{aligned} \tag{4.1}$$

where the functions f and g are as specified in (3.1) and (3.2). Assuming



(a) Schematic diagram



(b) In-plane elevation of cable 5

Fig. 4.1 - Two-buoy System

that end 1 is fixed, the stiffness matrix relating the increments in forces at end 2 to the increments of displacements at this end (in the directions  $x_1$ ,  $x_2$  and  $x_3$ ) is

$$\begin{aligned} \tilde{K}_{22} &= \begin{bmatrix} k_{11} & 0 & k_{13} \\ 0 & k_{22} & 0 \\ k_{31} & 0 & k_{33} \end{bmatrix} \\ &= \frac{1}{D} \begin{bmatrix} \frac{\partial g}{\partial V} & 0 & -\frac{\partial f}{\partial V} \\ 0 & D \frac{H}{\ell_5} & 0 \\ -\frac{\partial g}{\partial H} & 0 & \frac{\partial f}{\partial H} \end{bmatrix} \end{aligned} \quad (4.2)$$

where  $D = \frac{\partial f}{\partial H} \cdot \frac{\partial g}{\partial V} - \frac{\partial f}{\partial V} \cdot \frac{\partial g}{\partial H}$  and each of the functions  $\frac{\partial f}{\partial H}$  etc. are evaluated at  $(H, V)$ . Considerations of the equilibrium of the cable gives the stiffness matrix relating the increments in forces at end 1 to the increments of displacements of end 2 as

$$\tilde{K}_{12} = -\tilde{K}_{22} \quad (4.3)$$

The corresponding stiffness matrices for small displacements of end 1 can be obtained by rewriting the equations of (4.1) in terms of the forces at this end,  $H'$  and  $V'$ . From equilibrium  $H = H'$  and  $V = W - V'$ , where  $W$  is the total weight of the cable. Substituting for  $H$  and  $V$  in the specific forms of the functions  $f$  and  $g$ , the following result is obtained:

$$\begin{aligned} \ell_5 &= f(H', W - V') = f(H', V') \\ h_5 &= g(H', W - V') = -g(H', V') \end{aligned} \quad (4.4)$$

The function  $f(H, V)$  and  $g(H, V)$  also have the following properties:

$$\begin{aligned} \frac{\partial f}{\partial H}(H, V) &= \frac{\partial f}{\partial H}(H', V') ; & \frac{\partial f}{\partial V}(H, V) &= - \frac{\partial f}{\partial V}(H', V') \\ \frac{\partial g}{\partial H}(H, V) &= - \frac{\partial g}{\partial H}(H', V') ; & \frac{\partial g}{\partial V}(H, V) &= \frac{\partial g}{\partial V}(H', V') \end{aligned} \quad (4.5)$$

where  $\frac{\partial f}{\partial H}(H, V)$  means that the function  $\frac{\partial f}{\partial H}$  is evaluated at  $(H, V)$ , etc.

By using the above identities and performing the necessary coordinate transformation (since  $H'$  is in the negative  $x_1$  direction), the stiffness matrix relating the increments in the forces at end 1 to increments in the  $x_1, x_2$  and  $x_3$  displacements at end 1 can be shown to be

$$\tilde{K}_{11} = \begin{bmatrix} k_{11} & 0 & -k_{13} \\ 0 & k_{22} & 0 \\ k_{31} & 0 & -k_{33} \end{bmatrix} \quad (4.6)$$

where  $k_{11}, k_{12}$  etc. are the same values as in (4.2). The stiffness matrix relating the increments in forces at end 2 to the increments in displacements of end 1 is

$$\tilde{K}_{21} = - \tilde{K}_{11} \quad (4.7)$$

Let  $R$  be the rotation matrix describing the transformation of the  $(x_1, x_2, x_3)$  coordinate system to the  $(x, y, z)$  coordinate system, and let

$$\begin{aligned} \tilde{K}_1^5 &= R^T \tilde{K}_{11} R \\ \text{and} \quad \tilde{K}_2^5 &= R^T \tilde{K}_{22} R \end{aligned} \quad (4.8)$$

Noting that  $\tilde{K}^i$  stands for the tangent stiffness matrix of cable  $i$  ( $i = 1, 2, 3, 4$ ) in the global  $(x, y, z)$  coordinate system, the  $6 \times 6$  tangent stiffness matrix of the entire system is

$$\tilde{K} = \begin{bmatrix} (\tilde{K}^1 + \tilde{K}^2 + \tilde{K}_1^5) & -\tilde{K}_2^5 \\ -\tilde{K}_1^5 & (\tilde{K}^3 + \tilde{K}^4 + \tilde{K}_2^5) \end{bmatrix} \quad (4.9)$$

The static solution procedure is essentially the same as that described in Chapter 3. The iterative formula is (see equation 3.14)

$$\tilde{u}_n = \tilde{u}_{n-1} + \tilde{K}_{n-1}^{-1} (\tilde{Q}_A - \tilde{Q}_{n-1}) \quad (4.10)$$

For large matrices  $\tilde{K}$  the inversion required above may be more efficiently done by first solving the system of linear simultaneous equations

$$\tilde{K}_{n-1} \Delta \tilde{u}_{n-1} = \tilde{Q}_A - \tilde{Q}_{n-1}$$

to find  $\Delta \tilde{u}_{n-1}$  and then obtaining

$$\tilde{u}_n = \tilde{u}_{n-1} + \Delta \tilde{u}_{n-1} .$$

#### 4.2 Moored Semisubmersibles

The static analysis of a moored semisubmersible is in general difficult due to the deformation of the structure itself under the buoyancy forces and the forces applied by the cables. An iterative tangent stiffness solution procedure can be readily applied to the problem if the semisubmersible is assumed to be rigid.

Consider a rectangular semisubmersible attached to the seabed by four clusters of cables as illustrated in Fig. 4.2. Let the tangent stiffness matrix of each cable cluster corresponding to increments of the x, y and z displacements of the apex of the cluster be

$$\tilde{K}^i = \begin{bmatrix} k_{11}^i & k_{12}^i & k_{13}^i \\ k_{21}^i & k_{22}^i & k_{23}^i \\ k_{31}^i & k_{32}^i & k_{33}^i \end{bmatrix} ; \quad i = 1, 2, 3, 4 \quad (4.11)$$

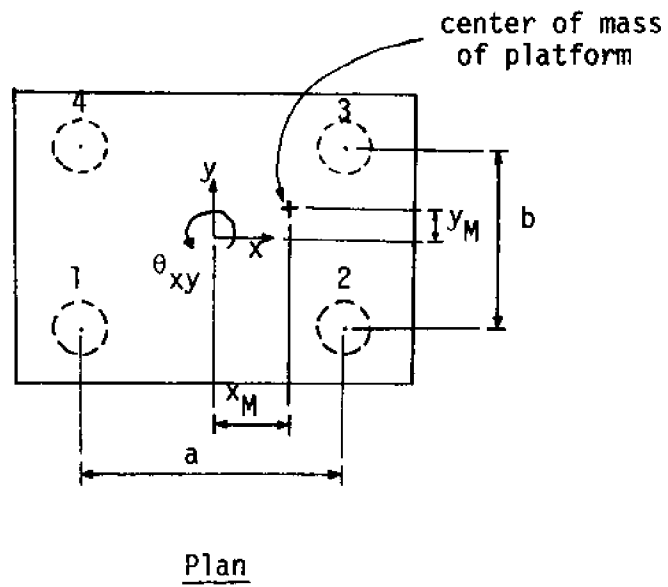
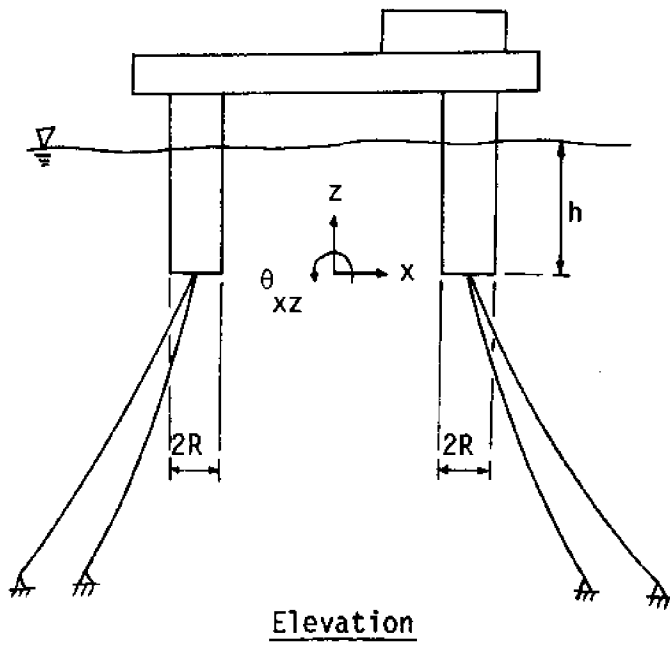


Fig. 4.2 - Rectangular Moored Semisubmersible

The complete system has six degrees of freedom, corresponding to the three displacements  $u, v, w$  and the three rotations,  $\theta_{xz}, \theta_{yz}, \theta_{xy}$  of the rigid semisubmersible. The  $6 \times 6$  tangent stiffness matrix, due to the stiffnesses of the four clusters only (i.e., neglecting, for the moment, the bouyancy effects on the semisubmersible), can be easily assembled using the tangent stiffness matrix of each cluster. For example, a small rotation  $d\theta_{xz}$  lowers the points 1 and 4 and raises the points 2 and 3 by  $\frac{a}{2} d\theta_{xz}$ . The stiffness terms corresponding to this rotation are the coefficients of  $d\theta_{xz}$  in the forces  $F_x, F_y, F_z$  and moments  $M_{xz}, M_{yz}, M_{xy}$  required to obtain this rotation while all the remaining displacements and rotations are maintained at zero. The assembled tangent stiffness matrix is

$$\underline{k}_c = [k_{ij}^c] \quad , \quad i = 1 \text{ to } 6, j = 1 \text{ to } 6 \quad (4.12)$$

where

$$k_{ij}^c = \left\{ \begin{array}{l} \sum_{n=1}^4 k_{ij}^n \quad \left\{ \begin{array}{l} i=1,2,3; j=1,2,3 \\ i=4; j=1,2,3; p=3; q=j \\ i=1,2,3; j=4; p=i; q=3 \end{array} \right. \\ \frac{a}{2} (-k_{pq}^1 + k_{pq}^2 + k_{pq}^3 - k_{pq}^4) \\ \frac{b}{2} (-k_{pq} - k_{pq}^2 + k_{pq}^3 + k_{pq}^4) \quad \left\{ \begin{array}{l} i=5; j=1,2,3; p=3; q=j \\ i=1,2,3; j=5; p=i; q=3 \end{array} \right. \\ \left[ \frac{a}{2} (-k_{pq}^1 + k_{pq}^2 + k_{pq}^3 - k_{pq}^4) \right. \\ \left. + \frac{b}{2} (k_{rs}^1 + k_{rs}^2 - k_{rs}^3 - k_{rs}^4) \right] \quad \left\{ \begin{array}{l} i=6; j=1,2,3; p=2; q=s=j; r=1 \\ i=1,2,3; j=6; p=r=i; q=2; s=1 \end{array} \right. \\ \left[ \frac{a^2}{4} \sum_{n=1}^4 k_{pq}^n \right. \\ \left. + \frac{ab}{4} (-k_{rs}^1 + k_{rs}^2 - k_{rs}^3 + k_{rs}^4) \right] \quad \left\{ \begin{array}{l} i=4; j=6; p=r=3; q=2; s=1 \\ i=6; j=4; p=2; q=s=3; r=1 \end{array} \right. \\ \left[ \frac{ab}{4} (k_{pq}^1 - k_{pq}^2 + k_{pq}^3 - k_{pq}^4) \right. \\ \left. - \frac{b^2}{4} \sum_{n=1}^4 k_{rs}^n \right] \quad \left\{ \begin{array}{l} i=5; j=6; p=r=3; q=2; s=1 \\ i=6; j=5; p=2; q=s=3; r=1 \end{array} \right. \end{array} \right.$$

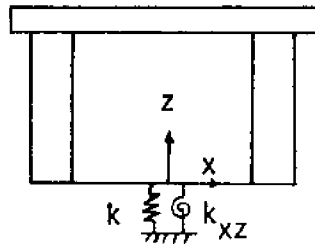
$$\begin{aligned}
 & \frac{a^2}{4} (-k_{33}^1 + k_{33}^2 + k_{33}^3 - k_{33}^4) & i = j = 4 \\
 & \frac{b^2}{4} (-k_{33}^1 - k_{33}^2 + k_{33}^3 + k_{33}^4) & i = j = 5 \\
 & \left[ \frac{a^2}{4} \sum_{n=1}^4 k_{22}^n + \frac{b^2}{4} \sum_{n=1}^4 k_{11}^n \right. & i = j = 6 \\
 & \left. + \frac{ab}{4} (-k_{12}^1 - k_{21}^1 + k_{12}^2 + k_{21}^2 - k_{12}^3 - k_{21}^3 + k_{12}^4 + k_{21}^4) \right]
 \end{aligned}$$

Buoyancy effects on the rigid semisubmersible

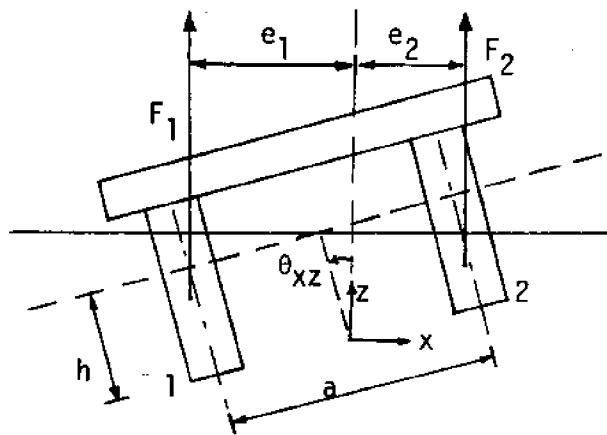
If the vertical upward buoyancy force on the platform in the initial rest position is included in the externally applied loads, the excess buoyancy forces and moments due to displacement of the rigid semisubmersible can be accounted for by replacing the water by equivalent springs as shown in Fig. 4.3(a). In the following derivations, the rotations  $\theta_{xz}$  and  $\theta_{yz}$  of the platform are assumed to be small so that  $\cos \theta \approx 1$  and  $\sin \theta \approx \theta$ . As a result of this assumption, the forces and moments exerted on the platform by buoyancy effects are linearly related to the corresponding displacements and rotations.

Consider again the four-legged semisubmersible shown in Fig. 4.2. The legs of the semisubmersible are cylindrical with radius R. The deck is assumed to be sufficiently clear of the water so that it will never submerge. Displacements and rotation in the horizontal plane ( $u, v$  and  $\theta_{xy}$ ) do not result in any excess buoyancy forces. A vertical upward displacement of  $w$  results in an excess force  $F_z = -4\pi\gamma R^2 w$ , where  $\gamma$  is the unit weight of the water. The effects of rotation are slightly more complex. Fig. 4.3(b) shows the semisubmersible under a rotation  $\theta_{xz}$ . The net buoyancy force from the two legs to the left of the origin is  $F_1$ , while the force from the other two legs is  $F_2$ . The distances to the line of action of these forces from the z-axis are  $e_1$  and  $e_2$  respectively. The buoyancy forces act through the center of volume of the submerged part

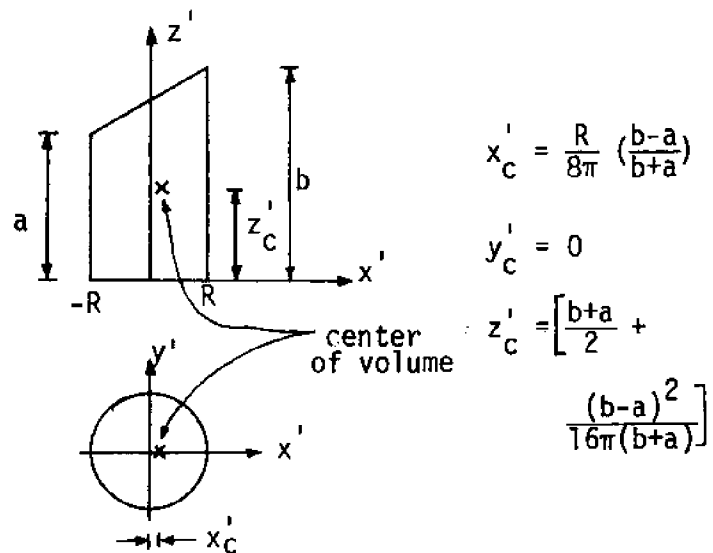




(a) Equivalent model accounting for excess buoyancy forces



(b) Semisubmersible rotated about the origin



(c) Center of volume of immersed portion of leg

Fig. 4.3 - Buoyancy Effects on the Semisubmersible

of the legs. Using the coordinates of the center of volume given in Fig. 4.2(c), and assuming that  $\theta_{xz}$  is small,

$$\begin{aligned} F_1 &= \pi R^2 \gamma (2h + a\theta_{xz}) \\ F_2 &= \pi R^2 \gamma (2h - a\theta_{xz}) \end{aligned} \quad (4.13)$$

The resultant counterclockwise moment about the origin is

$$\begin{aligned} M_{xz} &= -F_1 e_1 + F_2 e_2 \\ &= -F_1 \left[ \frac{a}{2} + \frac{R}{8\pi} \left( \frac{2R\theta_{xz}}{2h + a\theta_{xz}} \right) \right] + F_2 \left[ \frac{a}{2} - \frac{R}{8\pi} \left( \frac{2R\theta_{xz}}{2h - a\theta_{xz}} \right) \right] \\ &= - \left[ \frac{1}{2} + \pi \left( \frac{a}{R} \right)^2 \right] \gamma R^4 \end{aligned}$$

Prior to the imposed rotation the net buoyancy force was  $\pi R^2 \gamma$  and the moment of this force about the origin was zero. Thus the excess buoyancy force on the semisubmersible due to the rotation  $\theta_{xz}$  is zero and the excess moment is  $M_{xz}$ . Similarly for a rotation  $\theta_{yz}$ , the excess moment due to buoyancy is

$$M_{yz} = - \left[ \frac{1}{2} + \pi \left( \frac{b}{R} \right)^2 \right] \gamma R^4$$

From the above results it can be seen that for the model illustrations in Fig. 4.3(a) the translational spring has a stiffness  $k = 4\pi\gamma R^2$  and the rotational springs have stiffnesses  $k_{xz} = \left[ \frac{1}{2} + \pi \left( \frac{a}{R} \right)^2 \right] \gamma R^4$  and  $k_{yz} = \left[ \frac{1}{2} + \pi \left( \frac{b}{R} \right)^2 \right] \gamma R^4$ . The force-displacement relations due to the excess buoyancy effects can be described by means of the diagonal stiffness matrix (corresponding to  $u, v, w, \theta_{xz}, \theta_{yz}, \theta_{xy}$ )

$$\underline{K}_B = [k_{ij}^B] \quad , \quad i = 1 \text{ to } 6, \quad j = 1 \text{ to } 6 \quad (4.18)$$

where

$$k_{33}^B = -k$$

$$k_{44}^B = -k_{xz}$$

$$k_{55}^B = -k_{yz}$$

and all other  $k_{ij}^B$  are zero.

Analysis procedure

A suitable analysis procedure is, again, the tangent stiffness technique described in Chapter 3. The tangent stiffness matrix of the complete system is

$$\underline{K} = \underline{K}_C + \underline{K}_B \quad (4.19)$$

where  $\underline{K}^C$  and  $\underline{K}^B$  are as given in (4.12) and (4.18). The iterative formula to be used is

$$\underline{u}_n = \underline{u}_{n-1} + \Delta \underline{u}_{n-1} \quad (4.20)$$

where  $\Delta \underline{u}_{n-1}$  is the solution of

$$\underline{K}_{n-1} \Delta \underline{u}_{n-1} = \underline{Q}_A - \underline{Q}_{n-1}$$

(Note that  $\underline{u}^T = (u, v, w, \theta_{xz}, \theta_{yz}, \theta_{xy})$ ).

If the total weight of the platform is  $W$ , the  $x$  and  $y$  coordinates of the center of mass is  $x_M$  and  $y_M$ , the initial submerged length of the legs is  $h$  (see Fig. 4.2), the components of the current drag force in the  $x$  and  $y$  directions is  $F_x$  and  $F_y$ , and the horizontal twisting moment due to eccentricity of the drag forces is  $M_{xy}$ , then the (constant) applied force vector is

$$\underline{Q}_A = \begin{Bmatrix} F_x \\ F_y \\ 4\pi R^2 \gamma h - W \\ -W x_M \\ -W y_M \\ M_{xy} \end{Bmatrix} \quad (4.21)$$

If the x, y and z components of the force required to hold each cluster at the configuration described by  $u_{n-1}$  is  $P_x^i, P_y^i, P_z^i$  ( $i=1,2,3,4$ ), (computed as in Chapter 3), then

$$Q_{n-1} = \begin{pmatrix} \sum_{i=1}^4 P_x^i \\ \sum_{i=1}^4 P_y^i \\ \sum_{i=1}^4 P_z^i \\ \frac{a}{2} (-P_z^1 + P_z^2 + P_z^3 - P_z^4) \\ \frac{b}{2} (-P_z^1 - P_z^2 + P_z^3 + P_z^4) \\ \left[ \frac{a}{2} (P_x^1 + P_x^2 - P_x^3 - P_x^4) \right. \\ \left. + \frac{b}{2} (-P_y^1 + P_y^2 + P_y^3 - P_y^4) \right] \end{pmatrix} + K_B u_{n-1} \quad (4.22)$$

Thus, at each step of the iteration  $Q_A - Q_{n-1}$  represents the unbalanced load.

REFERENCES

1. Berteaux, H.O., Buoy Engineering, John Wiley & Sons, 1976.
2. Goodman, T.R. and Breslin, J.P., "Statics and Dynamics of Anchoring Cables in Waves," Journal of Hydronautics, Vol. 10, No. 4, October 1976.
3. Huston, R.L. and Kamman, J.W., "A Representation of Fluid Forces in Finite Segment Cable Models," International Journal of Computers and Structures, Vol. 14, No. 3-4, pp. 281-287, 1981.
4. Irvine, H.M., Cable Structures, MIT Press, 1981.
5. Simpson, A. and Tabarrok, B., "On the Equilibrium Configuration of a Chain Subjected to Uniform Fluid Flow in a Horizontal Plane," International Journal of Mechanical Science, Vol. 18, pp. 91-94, 1976.
6. Skop, R.A. and O'Hara, G.J., "The Method of Imaginary Reactions," MTS Journal, Vol. 4, No. 1, Jan-Feb. 1970.

APPENDIX A

A DESIGN PROCEDURE FOR MULTI-LEG CABLE-BUOY SYSTEMS

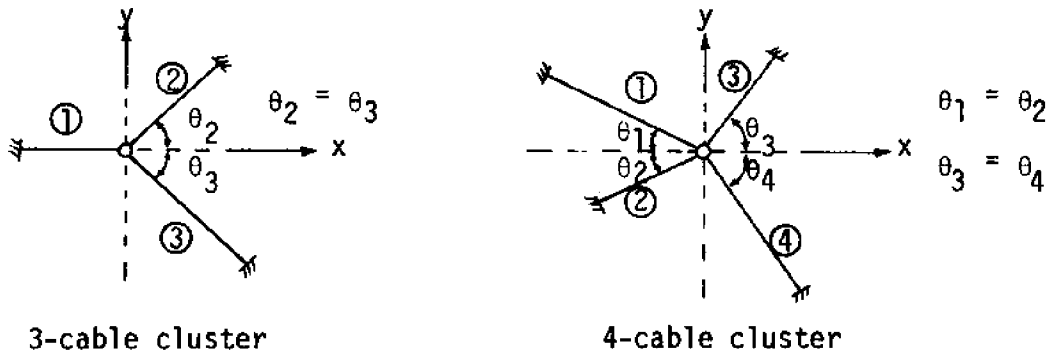
Outline of the Problem

The design problem of a submerged (or surface-moored) buoy usually consists of determining suitable dimensions for the mooring cables, and the locations of anchor points in the seabed, such that the buoy is located at a specified position (typically in a null current). Additional constraints are that the maximum stresses in the cables and the excursion of the buoy from the initial position should be within allowable limits under the design current (and wave) conditions.

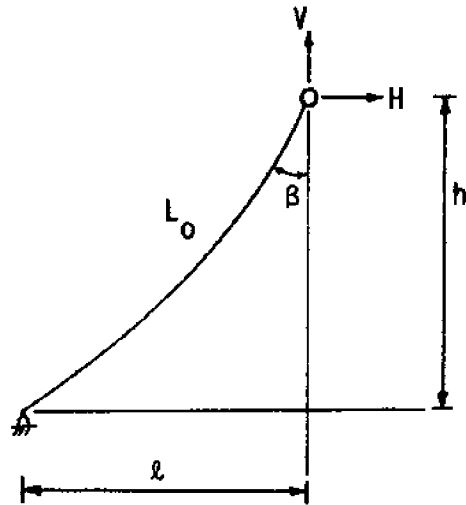
This chapter deals with the preliminary design problem of obtaining the dimensions of the mooring cables and the location of the anchor points. Estimates of the excursion of the buoy and the maximum stresses in the cables under design loads can then be obtained using the static analysis procedure discussed in Chapter 3, to check whether the constraints are satisfied. It should be noted that maximum cable stresses are sometimes attained under dynamic excitation, and hence a dynamic analysis of the system should also be performed. If the system does not satisfy the design constraints, then it needs to be redesigned with larger cables and/or a different cable arrangement, resulting in greater lateral stiffness.

A Preliminary Design Procedure

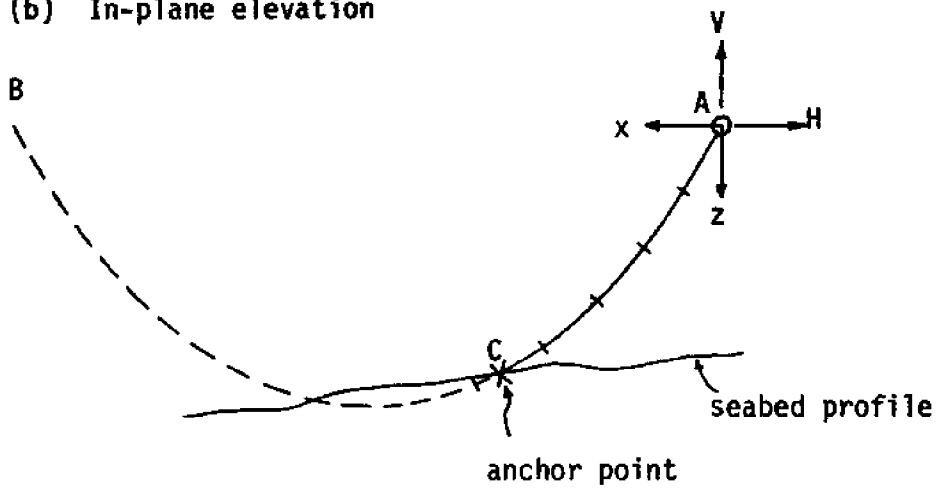
The design procedure suggested here relies on having cable arrangements that possess some symmetry, in plan view, about a horizontal x-axis (the direction of the dominant current, say). Fig. A-1(a) shows the plan views of two typical cable arrangements. The cables below the x-axis lie along the lines of reflection (about the x-axis) of the cables above the x-axis. Further, all the cables on the left side of the y-axis (group 1) are restricted to have the same cross-sectional area  $A_1$ , end forces  $V_1$  and  $H_1$  (and hence also the angle  $\beta_1 = \tan^{-1} H_1/V_1$ ) (See Fig. 5.1(b)), Young's modulus  $E_1$  and Poisson's ratio  $\nu_1$ , while the cables on the right side of the y-axis (group 2) have corresponding quantities  $A_2$ ,  $V_2$ ,  $H_2$ ,



(a) Typical cable arrangements - plan view



(b) In-plane elevation



(c) The profile and anchor point

Fig. A.1 - Definition Diagrams for Typical Cables

$\beta_2$ ,  $E_2$  and  $v_2$ . Due to this particular arrangement, equilibrium of the buoy in the y-direction is ensured.

The design procedure now consists of the following steps.

- 1) Choose the plan angles of the cables on one side of the x-axis and the ratio  $V_1/V_2$ . (These choices will usually be influenced by the directions and magnitudes of dominant currents and waves).
- 2) Choose the angle  $\beta_1$  and determine  $\beta_2$  so that equilibrium is satisfied in the z-direction. For example, in the four-cable cluster of Fig. A-1(a), the angle  $\beta_2$  (for cables 3 and 4) is related to  $\beta_1$  by

$$\beta_2 = \tan^{-1} \left\{ \frac{V_2}{V_1} \left( \frac{\cos \theta_3 + \cos \theta_4}{\cos \theta_1 + \cos \theta_2} \right) \tan \beta_1 \right\} \quad (A1)$$

- 3) Using the maximum cable tensions  $T_i = \frac{V_i}{\cos \beta_i}$  ( $i = 1, 2$ ), determine suitable cable cross-sections.
- 4) The end forces  $V$  and  $H$  and the cable properties define the catenary profile of each cable. Check that all profiles intersect the seabed. The point of intersection of the cable profile and the seabed is the anchor point for each cable. If any profile does not intersect the seabed, then that profile is too shallow. Decrease  $\beta_1$  and repeat steps 2 to 4 until all cables intersect the seabed.

In determining the anchor points in step 4 above, a numerical procedure is required. Let a cable under consideration have self-weight  $w$  per unit length, Young's modulus  $E$  and cross-sectional area  $A$ . Referring to Fig. A-1(a), let the curve length  $AB$  be  $L$  and  $AC$  be  $L_0$ . If the end forces of  $A$  are  $H$  and  $V$ , then the cable profile in terms of the unstrained Lagrangian coordinate  $s$  is described by

$$\begin{aligned} x(s) &= \frac{Hs}{EA_0} + \frac{H}{w} \left[ \sinh^{-1} \left( \frac{V}{H} \right) - \sinh^{-1} \left( \frac{V - ws}{H} \right) \right] \\ z(x) &= \frac{s}{EA_0} \left( V - \frac{ws}{2} \right) \\ &+ \frac{H}{w} \left[ \left\{ 1 + \left( \frac{V}{H} \right)^2 \right\}^{1/2} - \left\{ 1 + \left( \frac{V - ws}{H} \right)^2 \right\}^{1/2} \right] \end{aligned} \quad (A2)$$



The curve length AB is  $L = \frac{2V}{w}$ . If the seabed profile beneath the cable is given by  $z_s(x)$ , then by successively checking  $z - z_s$  for  $s = n\Delta s$ ,  $n = 1, 2, \dots$  ( $\Delta s = \frac{L}{100}$  say), the interval in which the profile intersects the seabed can be determined. By successive bisections within this interval, the location of the anchor point can be estimated to the required level of accuracy.

Note that this design procedure may not give the most economical solution, but it enables the buoy to be positioned (in a null current) at a fixed location. It should be recognized, however, that accurate positioning in the offshore environment is often a difficult task and reasonable accuracy is all that can be expected.

APPENDIX B - A FORTRAN COMPUTER PROGRAM

Listing of Program

Sample Output from Program

APPENDIX B - Listing of Program

```

C *** NONLINEAR ANALYSIS OF A BUOY ANCHORED BY A CABLE SYSTEM
C *** USING A TANGENT STIFFNESS ITERATIVE TECHNIQUE.
C *** WRITTEN BY RONALD HARICHANDRAN
C *** INITIATION DATE 10/1/81
C
C *** INPUT VARIABLE DESCRIPTION
C *** NOTE - ALL ANGLES ARE TO BE IN DEGREES AND MEASURED COUNTERCLOCKWISE
C *** FROM THE X-AXIS
C - THE Z-AXIS IS TO BE DIRECTED UPWARD
C - INPUT ALL DATA IN THE ORDER AND FORMAT INDICATED BY THE READ
C STATEMENTS
C
C * N = NO. OF CABLES (MAXIMUM=8)
C * E(I),A(I),W(I) = YOUNG'S MODULUS AND CROSS-SECTIONAL AREA AND
C SUBMERGED WEIGHT PER UNIT LENGTH FOR CABLE I
C
C * IB = 2 FOR SURFACE-MOORED BUOYS
C * = 3 FOR SUBMERGED BUOYS
C
C * BF = SUBMERGED BUOYANT FORCE
C * ZF = Z-ORDINATE OF THE FREE SURFACE OF THE SEA (USED ONLY IN COMPUTING
C THE ACTUAL STRESSES IN THE CABLE)
C * G = ACCELERATION UNDER GRAVITY
C * RO = DENSITY OF SEA WATER
C * H(I) = HORIZONTAL EFFECTIVE FORCE AT UPPER END OF CABLE I
C (IF UNKNOWN TRY AN INITIAL GUESS)
C * V(I) = VERTICAL EFFECTIVE FORCE AT UPPER END OF CABLE I
C (IF UNKNOWN TRY AN INITIAL GUESS)
C
C * XB,YB,ZB = COORDINATES OF BUOY
C * XA(1),YA(1),ZA(1) = COORDINATES OF SEARED ANCHOR POINTS
C * LB(I) = LENGTH OF CABLE I
C * O(3) = VECTOR OF THE X,Y AND Z COMPONENTS OF THE DRAG FORCE ON THE BUOY
C * ICUR = 0 IF CURRENT DRAG ON CABLES IS NOT REQUIRED TO BE COMPUTED
C * = 1 IF CURRENT DRAG ON CABLES IS TO BE COMPUTED
C
C *** IF ICUR=1 USE THE EQUILIBRIUM POSITION OF THE BUOY WITHOUT CURRENT
C FORCES AS INITIAL POSITION. THE FOLLOWING DATA IS ALSO REQUIRED.
C
C * D(I) = DIAMETER OF CABLE I
C * VEL = MAGNITUDE OF CURRENT VELOCITY
C * VDIR = ANGLE SPECIFYING THE DIRECTION OF THE CURRENT
C * CD = DRAG COEFFICIENT FOR THE CABLES
C
C
C REAL XA(8),YA(8),ZA(8),F(3,3),Z(8),A(8),LA(8),H(8),
C V(8),O(3),OI(3),B(3),W(8),PLANA(8),PFB(8),BL(3),D(8)
C COMMON/SF/XA,YA,ZA,F,E,A,N,LB,XB,YB,ZB,PLANA,H,V,B,IS
C COMMON/IT/NITER
C COMMON/E/CD,D,RO,VEL,VDIR,O
C EQUIVALENCE (B(1),XB),(B(2),YB),(B(3),ZB)
C
C * READ INPUT DATA
C
C
C WRITE(6,1000)
C FORMAT(5X,'*** INPUT DATA ***,/')
C READ(5,*)N
C WRITE(6,1100)
C FORMAT(/,5X,'MATERIAL PROPERTIES')

```

```
DO 1 I=1,N
  READ(5,*)E(I),A(I),W(I)
  WRITE(6,1200)I,E(I),A(I),W(I)
  FORMAT(5X,'CABLE',I3,5X,'E',E10.4,5X,'A',A10.4,5X,
        'W',E10.4)
C
  READ(5,*)IB,8F
  WRITE(6,1400)8F
  FORMAT(/,5X,'SUBMERGED BUOYANT FORCE =',E15.5)
C
  READ(5,*)ZF,G,RO
  WRITE(6,1450)ZF,G,RO
  FORMAT(/,5X,'Z-ORDINATE OF THE FREE SURFACE =',E15.5,/,
        5X,'ACCELERATION UNDER GRAVITY =',E15.5,/,
        5X,'DENSITY OF SEA WATER =',E15.5)
C
  READ(5,*)(H(I),I=1,N)
  READ(5,*)(V(I),I=1,N)
  WRITE(6,1300)(I,H(I),V(I),I=1,N)
  FORMAT(/,5X,'GUESSES FOR HORIZONTAL AND VERTICAL FORCES AT',
        'UPPER END OF EACH CABLE',/,48*(5X,'CABLE',I3,5X,
        'H =',E15.5,5X,'V =',E15.5,/)
C
  READ(5,*)(XB,YB,ZB)
  WRITE(6,1500)XB,YB,ZB
  FORMAT(/,5X,'COORDINATES OF BUOY',/,5X,(' ',3E15.5,')')
C
  WRITE(6,1600)
  FORMAT(/,5X,'COORDINATES OF ANCHOR POINTS AND CABLE LENGTHS',/,
        5X,'CABLE',20X,'COORDINATES',33X,'LENGTH')
  DO 3 I=1,N
    READ(5,*)(XA(I),YA(I),ZA(I),L0(I))
    WRITE(6,1700)I,XA(I),YA(I),ZA(I),L0(I)
    FORMAT(5X,I3,5X,(' ',3E15.5,')',E20.5)
C
  READ(5,*)(Q(I),I=1,3)
  WRITE(6,1800)(Q(I),I=1,3)
  FORMAT(/,5X,'X,Y AND Z COMPONENTS OF DRAG FORCE ON BUOY',/,5X,
        (' ',3E15.5,')')
C
  READ(5,*)ICUR
  IF(ICUR.NE.1)GO TO 5
C
  READ(5,*)(D(I),I=1,N)
  WRITE(6,1820)(D(I),I=1,N)
  FORMAT(/,5X,'CABLE DIAMETERS',/,5X,<N>P10.4)
C
  READ(5,*)VEL,VDIR,CD
  WRITE(6,1830)VEL,VDIR,CD
  FORMAT(/,5X,'MAGNITUDE OF CURRENT VELOCITY =',E15.5,
        10X,'DIRECTION OF CURRENT VELOCITY =',E15.5,
        /,5X,'DRAG COEFFICIENT FOR ALL CABLES =',E15.5)
C
  WRITE(6,1900)
  FORMAT(/,5X,'**** OUTPUT ****',/)
```

```
C
10 DO 10 I=1,18
   QI(I)=0.0
   QINC=1.0
   NITER=0
   IER=1
C * LET Q BE THE TOTAL FORCE APPLIED AT THE BUOY
C
C Q(3)=BF
C * COMPUTE TANGENT FLEXIBILITY MATRIX OF CABLE SYSTEM
C
C CALL FLEX(IER)
   IER=0
   IF(ICUR.EQ.1)CALL EQUIV
C DO 20 I=1,100
C * COMPUTE ESTIMATED POSITION OF BUOY
C
C DO 30 K=1,18
   BL(K)=B(K)
C DO 30 J=1,18
   B(K)=B(K)+F(K,J)*(Q(J)-QI(J))*QINC
C * CHECK FOR CONVERGENCE - ALLOW 1% ERROR IN TOTAL MAGNITUDE OF FORCE
C
C QM=0.0
   DQM=0.0
   DO 40 J=1,18
     QM=QM+Q(J)*Q(J)
     DQM=DQM+(Q(J)-QI(J))**2
     QM=SQRT(QM)
     DQM=SQRT(DQM)
     IF((DQM/QM).LE.0.01)GO TO 70
C * COMPUTE THE REAL FORCE REQUIRED TO PRODUCE THE ESTIMATED DISPLACEMENT.
C ALSO COMPUTE THE NEW FLEXIBILITY MATRIX.
C
C CALL FLEX(IER)
   IF(IER.NE.99)GO TO 45
C * IF SUBROUTINE "FORCES" DID NOT CONVERGE DUE TO POOR INITIAL GUESSES FOR
C CABLE FORCES, HALVE THE APPLIED LOAD INCREMENT AND TRY AGAIN
C
C QINC=QINC/2
   B(1)=BL(1)
   B(2)=BL(2)
   B(3)=BL(3)
   GO TO 25
C
C QINC=1.0
C * QI IS THE FORCE REQUIRED TO HOLD CABLE CLUSTER AT THE CURRENT POSITION
```

```

C      QI(1)=0.0
C      QI(2)=0.0
C      QI(3)=0.0
C
C      DO 60 J=1,N
C
C      QI(1)=QI(1)+H(J)*COS(PLANA(J))
C      QI(2)=QI(2)+H(J)*SIN(PLANA(J))
C      QI(3)=QI(3)+V(J)
C      CONTINUE
C      CONTINUE
C
C      WRITE(6,2000)
C      FORMAT(/,5X,'THE NONLINEAR ANALYSIS FAILED TO CONVERGE',
C            /,5X,' IN 100 ITERATIONS')
C
C      WRITE(6,3000)XB,YB,ZB,Q(1),Q(2),Q(3),QI(1),QI(2),QI(3)
C      FORMAT(/,5X,'COORDINATES OF BUOY UNDER THE APPLIED LOAD',
C            /,5X,' ,',3E15.5,')',/,5X,'APPLIED FORCES AND ACTUAL',
C            /,5X,' ,',3E15.5,')',/,5X,'FORCES REQUIRED TO MAINTAIN BUOY AT ABOVE LOCATION',
C            /,2(5X,' ,',3E15.5,')')
C
C      * STORE MAXIMUM TENSILE STRESSES IN THE CABLES AT THE DISPLACED POSITION
C      IN ARRAY "PLANA" AND PRINT
C
C      WRITE(6,5100)
C      FORMAT(/,5X,'MAXIMUM CABLE STRESSES IN THE DISPLACED POSITION')
C      DO 80 J=1,N
C      TE=SQRT(H(J)*H(J)+V(J)*V(J))
C      PLANA(J)=TE/A(J)-RO*G*A(J)*(ZF-ZB)/(1+TE/E(J)/A(J))
C      WRITE(6,5000)J,PLANA(J)
C      FORMAT(5X,'CABLE',I3,5X,'STRESS =',E20.5)
C
C      WRITE(6,5500)
C      FORMAT(/,5X,'HORIZONTAL AND VERTICAL COMPONENTS OF EFFECTIVE',
C            /,5X,' FORCE (IN LOCAL COORDS.) AT THE UPPER END OF EACH CABLE',
C            /,5X,' AT THE DISPLACED POSITION')
C      DO 85 J=1,N
C      WRITE(6,5600)J,H(J),V(J)
C      FORMAT(5X,'CABLE',I3,5X,'H =',E15.5,5X,'V =',E15.5)
C
C      WRITE(6,6000)I,NITER
C      FORMAT(/,5X,'NUMBER OF ITERATIONS IN TANGENT STIFFNESS',
C            /,5X,' SOLUTION =',I5,/,5X,'TOTAL NO. OF ITERATIONS IN',
C            /,5X,' SOLUTION OF NONLINEAR SIMULTANEOUS EQNS. (INCLUDES',
C            /,5X,' ALL SOLNS. FOR ALL CABLES) =',I7)
C
C      IF(IB.EQ.2.AND.QI(3).GT.BF)WRITE(6,6500)
C      FORMAT(/,5X,'!!! ATTENTION !!!',/,5X,'VERTICAL PULL-DOWN',
C            /,5X,' FORCE DUE TO CABLES IS LARGER THAN THE SUBMERGED',
C            /,5X,' BUOYANT FORCE ON THE BUOY AND THE BUOY WILL',
C            /,5X,' SUBMERGE. THE ABOVE RESULTS DO NOT ALLOW FOR THIS.',
C            /,5X,' IF SUBMERGENCE IS TO BE ALLOWED FOR, REDEFINE',
C            /,5X,' THE PROBLEM AS A SUBMERGED BUOY PROBLEM.')
C
C      END

```



```
C * FORM 2X2 FLEXIBILITY MATRIX IN LOCAL COORDINATES
C
C1=V(I)/H(I)
C2=(V(I)-WT)/H(I)
C3=SQRT(1+C1*C1)
C4=SQRT(1+C2*C2)
C5=L0(I)/WT
C
F(1,1)=L0(I)/E(I)/A(I)+C5*(SINHI(C1)-SINHI(C2)-C1/C3+C2/C4)
F(1,2)=C5*(1/C3-1/C4)
F(2,1)=C5*(C3-C4-C1*C1/C3+C2*C2/C4)
F(2,2)=L0(I)/E(I)/A(I)+C5*(C1/C3-C2/C4)
D=F(1,1)*F(2,2)-F(1,2)*F(2,1)
C
DO 40 J=1,2
DO 40 JJ=1,2
F(J,J)=F(J,J)/D
C * COMPUTE OUT OF PLANE STIFFNESS OF CABLE
C
KD=H(I)/L
C=COS(PLANA(I))
S=SIN(PLANA(I))
C * COMPUTE STIFFNESS MATRIX OF SYSTEM
C
K(1,1)=K(1,1)+C*C*F(2,2)+S*S*KD
K(1,2)=K(1,2)+S*C*(F(2,2)-KD)
K(1,3)=K(1,3)-C*F(1,2)
K(2,1)=K(1,2)
K(2,2)=K(2,2)+S*S*F(2,2)+C*C*KD
K(2,3)=K(2,3)-S*F(1,2)
K(3,1)=K(3,1)-C*F(2,1)
K(3,2)=K(3,2)-S*F(2,1)
K(3,3)=K(3,3)+F(1,1)
C
CONTINUE
C 10
C * INVERT THE STIFFNESS MATRIX TO OBTAIN THE FLEXIBILITY MATRIX
C
IF(10-EO.2)GO TO 65
KD=K(1,1)*(K(2,2)*K(3,3)-K(2,3)*K(3,2))-
1 K(1,2)*(K(2,1)*K(3,3)-K(2,3)*K(3,1))+
1 K(1,3)*(K(2,1)*K(3,2)-K(2,2)*K(3,1))
FS(1,1)=(K(2,2)*K(3,3)-K(2,3)*K(3,2))/KD
FS(1,2)=-K(1,2)*K(3,3)+K(1,3)*K(3,2)/KD
FS(1,3)=-K(1,2)*K(2,3)+K(1,3)*K(2,2)/KD
FS(2,1)=-K(2,1)*K(3,3)+K(2,3)*K(3,1)/KD
FS(2,2)=-K(1,1)*K(3,3)+K(1,3)*K(3,1)/KD
FS(2,3)=-K(1,1)*K(2,3)+K(1,3)*K(2,1)/KD
FS(3,1)=-K(2,1)*K(3,2)+K(2,2)*K(3,1)/KD
```



```
FS(3,2)=-K(1,1)*K(3,2)-K(1,2)*K(3,1)/KD  
FS(3,3)=(K(1,1)*K(2,2)-K(1,2)*K(2,1))/KD
```

```
GO TO 70
```

```
* FOR SURFACE-MOORED BUOYS A 2X2 FLEXIBILITY MATRIX IS REQUIRED
```

```
KD=K(1,1)*K(2,2)-K(1,2)*K(2,1)
```

```
FS(1,1)=K(2,2)/KD
```

```
FS(1,2)=-K(1,2)/KD
```

```
FS(2,1)=-K(2,1)/KD
```

```
FS(2,2)=K(1,1)/KD
```

```
GO TO 70
```

```
* IF DIVERGENCE IS ENCOUNTERED IN SOLVING FOR ANY OF THE CABLE FORCES,  
RESET THE FORCES TO THE INITIAL VALUES THAT EXISTED BEFORE THE  
ATTEMPTED SOLUTION
```

```
DO 90 I=1,N
```

```
H(I)=HL(I)
```

```
V(I)=VL(I)
```

```
CONTINUE
```

```
RETURN
```

```
END
```

```
SUBROUTINE FORCES(N,L,HZ,L0,E,A,W,H,V,IRR)
```

```
* THIS SUBROUTINE DETERMINES THE CABLE FORCES FROM GIVEN GEOMETRY BY  
USING A 2-DIMENSIONAL NEWTON-RAPHSON SCHEME.
```

```
REAL L,L0
```

```
COMMON/IT/NITER
```

```
SINHI(X)=LOG(X+SQRT(1+X*X))
```

```
* USE EXISTING CABLE FORCES AS INITIAL GUESSES
```

```
DO 10 I=1,50
```

```
* COMPUTE FUNCTIONS F(H,V) AND G(H,V) AND PARTIAL DERIVATIVES.  
(SOLUTIONS H AND V SUCH THAT F(H,V)=0 AND G(H,V)=0 ARE REQUIRED)
```

```
C1=V/H
```

```
C2=(V-W)/H
```

```
C3=SQRT(1+C1*C1)
```

```
C4=SQRT(1+C2*C2)
```

```
C5=L0/W
```

```
C6=C5*(SINHI(C1)-SINHI(C2))
```

```
C7=L0/R/A
```

```
F=H*C7+H*C6-L
```

```
G=W*C7*(V/W-0.5)+H*C5*(C3-C4)-HZ
```

```
PX=C7+C6+C5*(-C1/C3+C2/C4)
```

```
FY=C5*(1/C3-1/C4)
GX=C5*(C3-C4)+C5*(-C1*C1/C3+C2*C2/C4)
GY=C7+C5*(C1/C3-C2/C4)
D=FX*GY-FY*GX
DHL=DH
DVL=DV
DH=(G*FY-F*GY)/D
DV=(F*GX-G*FX)/D
C * CHECK FOR DIVERGENCE FROM THE REQUIRED ROOT.
C
C
H=H+DH
V=V+DV
IF(H.LT.0.OR.V.LT.0)GO TO 30
C * ALLOW AN ERROR OF 0.1% IN H AND V
C
C
IF(ABS(DH/H).LE.0.001.AND.ABS(DV/V).LE.0.001)GO TO 40
CONTINUE
1000 WRITE(6,1000)N
FORMAT(//,5X,'NEWTON-RAPHSON ALGORITHM FOR CABLE',I3,
, FAILED TO CONVERGE IN 50 ITERATIONS')
C
C IF(IER.NE.1)GO TO 50
C
C IF THE USER SUPPLIED INITIAL GUESSES ARE NOT GOOD ENOUGH FOR
CONVERGENCE, STOP EXECUTION
C
C
WRITE(6,1100)N,H,V
FORMAT(//,5X,'1) INITIAL GUESS OF FORCES FOR CABLE',I3,' IS'
, POOR - TRY ANOTHER GUESS 11')
1100 STOP
C
C IER=99
C
C NITER=NITER+1
C
C RETURN
C
C EXD
C
C SUBROUTINE EQUIV
C
C *** THIS SUBROUTINE DETERMINES THE EQUIVALENT FORCES TO BE APPLIED AT
THE BUOY (IN ADDITION TO THE DRAG FORCE ON THE BUOY) DUE TO
DRAG ON THE CABLES.
C
C
REAL XA(8),YA(8),ZA(8),E(8),A(8),L0(8),R(8),V(8),
PS(3,3),W(8),PLANA(8),D(8),L,C(3)
COMMON/ST/XA,YA,ZA,PS,E,A,W,L0,XB,YB,ZB,PLANA,H,V,N,IB
COMMON/E/CD,D,RO,VEL,VDIR,Q
C
C PI=3.1415927
```

```
C
1000 WRITE(6,1000)
      FORMAT(/,/,5X,'EQUIVALENT LOAD AT BUOY DUE TO CURRENT DRAG ON',
            ' CABLES',/,5X,'CABLE',10X,
            ' EQUIVALENT LOAD (X,Y,Z COMPONENTS)')
C
C * PERFORM THE FOLLOWING STEPS FOR EACH CABLE
C
C DO 10 I=1,N
C
C * DETERMINE ANGLE OF CHORD TO HORIZONTAL AND THE FORCES AT THE TOP OF
C THE CABLE IN LOCALIZED COORDINATES PARALLEL AND PERPENDICULAR TO CHORD
C
      AA=ABS(ZB-ZA(I))
      B=SQRT((XB-XA(I))**2+(YB-YA(I))**2)
      THETA=ATAN(AA/B)
      C=COS(THETA)
      S=SIN(THETA)
      T=S/C
      L=SQRT(AA*AA+B*B)
      HT=H(I)*C+V(I)*S
      VT=H(I)*S+V(I)*C
C
C * DETERMINE FORCE ALONG AT THE BOTTOM END
C
      HB=HT-W(I)*L*S
C
C * DETERMINE THE IN-PLANE AND OUT-OF-PLANE UNIFORMLY DISTRIBUTED LOADS
C PERPENDICULAR TO THE CHORD
C
      VI=VEL*COS(PLANA(I)-VDIR)*S
      VO=VEL*SIN(PLANA(I)-VDIR)
      VI=RO/2*CD*D(I)*VI*ABS(VI)
      VO=RO/2*CD*D(I)*VO*VO
C
C * COMPUTE THE INCREASE IN TENSION DUE TO IN-PLANE LOAD
C
      G=HB/W(I)/L/S
      EE=2+1.0/(4*C*(G+1))-(1+2*G)*LOG(1+1/G)
      F=LOG(1+1/G)-(2+1/G)*(4*G*(G+1)-1)/8/G/(G+1)**2
      DELH=W*I*EE*T/(W(I)*L/E(I)/A(I)*T*S*F)
      HT=DELH
      VT=-WI*L/2
C
C * DETERMINE EQUIVALENT FORCES IN HORIZONTAL AND VERTICAL LOCALIZED
C COORDINATES
C
      HN=HT*C-VT*S
      VN=HT*S+VT*C
      HO=WO*L0(I)/2
      S=SIN(PLANA(I)+PI-VDIR)
      HO=HO*S/ABS(S)
C
C * TRANSFORM INTO GLOBAL COORDINATES AND ADD INTO FORCE VECTOR Q
C
```

```
S=SIN(PLANA(I))  
C=COS(PLANA(I))  
Q1=C*HN-S*HO  
Q2=S*HN+C*HO  
Q(1)=Q(1)+Q1  
Q(2)=Q(2)+Q2  
Q(3)=Q(3)+VN
```

```
C  
2000 WRITE(6,2000)I,Q1,Q2,VN  
C 10 FORMAT(5X,13,10K,1(' ',3E12.4,.''))  
CONTINUE  
RETURN  
END
```

Appendix B - Sample Output from Program

\*\*\* INPUT DATA \*\*\*

MATERIAL PROPERTIES  
 CABLE 1 E = 0.1724E+12 A = 0.1267E-03 W = 0.9760E+01  
 CABLE 2 E = 0.1724E+12 A = 0.1267E-03 W = 0.9760E+01  
 CABLE 3 E = 0.1724E+12 A = 0.1267E-03 W = 0.9760E+01

SUBMERGED BUOYANT FORCE = 0.9570E+05

Z-ORDINATE OF THE FREE SURFACE = 0.0000E+00  
 ACCELERATION UNDER GRAVITY = 0.9810E+01  
 DENSITY OF SEA WATER = 0.1020E+04

GUESSES FOR HORIZONTAL AND VERTICAL FORCES AT UPPER END OF EACH CABLE  
 CABLE 1 H = 0.1000E+03 V = 0.1000E+04  
 CABLE 2 H = 0.1000E+03 V = 0.1000E+04  
 CABLE 3 H = 0.1000E+03 V = 0.1000E+04

COORDINATES OF BUOY  
 ( -0.12178E+02 0.5232E+01 -0.21194E+03)

COORDINATES OF ANCHOR POINTS AND CABLE LENGTHS

CABLE	COORDINATES	LENGTH
1	( -0.1000E+03 0.0000E+00 -0.7050E+03)	0.5000E+03
2	( 0.5000E+02 0.86603E+02 -0.7020E+03)	0.5000E+03
3	( 0.5000E+02 -0.86603E+02 -0.7000E+03)	0.5000E+03

X, Y AND Z COMPONENTS OF DRAG FORCE ON BUOY  
 ( 0.2500E+04 0.0000E+00 0.0000E+00)

CABLE DIAMETERS  
 0.0127 0.0127 0.0127

MAGNITUDE OF CURRENT VELOCITY = 0.1000E+01 DIRECTION OF CURRENT VELOCITY = 0.0000E+00  
 DRAG COEFFICIENT FOR ALL CABLES = 0.7000E+00

\*\*\* OUTPUT \*\*\*

EQUIVALENT LOAD AT BUOY DUE TO CURRENT DRAG ON CABLES

CABLE	EQUIVALENT LOAD (X, Y, Z COMPONENTS)
1	( 0.6541E+03 0.3435E+02 -0.2571E+04)
2	( 0.6857E+03 -0.3863E+03 0.1667E+04)
3	( 0.5703E+03 0.5439E+03 0.2105E+04)

COORDINATES OF BUOY UNDER THE APPLIED LOAD = ( -0.10726E+02 0.52557E+01 -0.21191E+03)  
 APPLIED FORCES AND ACTUAL FORCES REQUIRED TO MAINTAIN BUOY AT ABOVE LOCATION  
 ( 0.43301E+04 0.19290E+03 0.96902E+05) ( 0.43277E+04 0.20044E+03 0.96951E+05)

MAXIMUM CABLE STRESSES IN THE DISPLACED POSITION  
CABLE 1 STRESS = 0.42375E+09  
CABLE 2 STRESS = 0.19417E+09  
CABLE 3 STRESS = 0.15974E+09

HORIZONTAL AND VERTICAL COMPONENTS OF EFFECTIVE FORCE (IN LOCAL COORDS.) AT THE UPPER END OF EACH CABLE  
AT THE DISPLACED POSITION

CABLE 1	H =	0.91654E+04	V =	0.52902E+05
CABLE 2	H =	0.44815E+04	V =	0.24189E+05
CABLE 3	H =	0.39017E+04	V =	0.19860E+05

NUMBER OF ITERATIONS IN TANGENT STIFFNESS SOLUTION = 4

TOTAL NO. OF ITERATIONS IN SOLUTION OF NONLINEAR SIMULTANEOUS EQNS. (INCLUDES ALL SOLNG. FOR ALL CABLES) = 68

